STRESS ANALYSIS OF SIMPLY AND MULTIPLY CONNECTED REGIONS CONTAINING CRACKS BY THE METHOD OF BOUNDARY COLLOCATION

By

J. C. Newman, Jr.

Thesis submitted to the Graduate Faculty of the

Virginia Polytechnic Institute

in candidacy for the degree of

MASTER OF SCIENCE

in

Engineering Mechanics

May 1969

STRESS ANALYSIS OF SIMPLY AND MULTIPLY CONNECTED REGIONS CONTAINING CRACKS BY THE METHOD OF BOUNDARY COLLOCATION

by

J. C. Newman, Jr.

Thesis submitted to the Graduate Faculty of the

Virginia Polytechnic Institute

in candidacy for the degree of

MASTER OF SCIENCE

in

Engineering Mechanics

APPROVED:

C. W. Smith

R. P. McNitt

H. F. Brinson

II. TABLE OF CONTENTS

III. ACKNOWLEDGMENTS

The author wishes to thank Professor C. W. Smith of Virginia Polytechnic Institute for his aid in the preparation of this thesis, , NASA-Langley Research Center, for her help in writing the computer programs, and the National Aeronautics and Space Administration for permission to publish the analysis as a thesis.

IV. LIST OF FIGURES

V. INTRODUCTION

Fatigue failures in structural components of aircraft, other vehicles, and machinery are caused by the initiation and cyclic growth of one or more cracks from areas of stress concentrations. The rates at which these cracks propagate and the maximum crack size at failure, depend primarily on the material, environmental conditions, structural configuration, and the type and magnitude of loading applied to the component. In the last decade, many investigators (for example, see refs. 1-3) have observed that a correlation exists between the crack tip stress-intensity factor and the rates of fatigue crack propagation in simple and complex specimens. Reference 3 has demonstrated that the stress-intensity solutions can be used to predict the crack propagation life of built-up structures. Therefore, a technique for calculating the stress-intensity factors for simply and multiply connected regions containing cracks should be useful to designers working in the fields of fatigue and fail-safe concepts.

Several investigators in the past two decades have obtained theoretical solutions for cracks growing in the vicinity of stress concentrations. For example, Bowie (ref. 4) presented the solution for radial cracks originating from a circular hole in an infinite plate subjected to a biaxial state of stress. Grebenkin and Kaminskii (ref. 5) have analyzed the propagation of cracks from the edge of a curvilinear hole in an infinite plate subjected to a biaxial state of stress. Erdogan (ref. 6) has presented the analysis for cracks in the vicinity of various notches in infinite and finite plates under longitudinal shear. Isida (ref. 7) has analyzed the case of a crack approaching a circular hole in an infinite plate subjected to a remote state of stress. References 4 through 6 employed a conformal mapping procedure to obtain the various solutions and reference 7 employed superposition of appropriate series stress functions to satisfy the stress conditions on the hole and crack boundary.

In the present investigation, theoretical stress analyses were performed for the case of cracks emanating from, or in the vicinity of holes or boundaries of various shapes in two-dimensional elastic bodies. The solution is based on the complex variable method developed by Muskhelishvili (ref. 8) and a numerical technique known as boundary collocation or point matching (ref. 9) for approximating the boundary conditions. Several techniques were used in the collocation method to approximate the boundary conditions and the results were compared in a few selected problems. These techniques included specifying boundary stresses at equally spaced points on the boundary, specifying the resultant forces along arcs on the boundary, and a least-squares technique developed in the text for minimizing the resultant force or displacement residuals along the boundary. The complex stress functions developed for simply and multiply connected regions containing cracks automatically satisfy the boundary conditions on the crack surfaces. The influence of the remaining boundaries on the crack tip stress-intensity factor for numerous boundary-value problems has been calculated. The types of configurations investigated included the case of cracks emanating from a circular hole, the case of a crack approaching and intersecting multiple-circular holes along the plane of the crack, the case of a crack propagating between multiple-circular holes where the centerline of the holes is perpendicular to the plane of the crack, and the case of cracks emanating from an elliptical hole. The configurations investigated were in an infinite plate and subjected to either internally or externally applied loads.

In the vicinity of stress concentrations, the local stresses may exceed the proportional limit of the material at some time in the loading history. In this situation, the local elastic solution becomes invalid and more elaborate elastic-plastic analyses are required to determine the local stresses and strains. In the past decade, Barenblatt (ref. 10) and Dugdale (ref. 11) have developed a simple model of yielding at the tip of a crack. Vitvitski and Leonov (ref. 12) have extended the model to the case of yielding at the edge of a circular hole. The Barenblatt-Dugdale model assumes that yielding occurs along a strip (wedge-shaped) in front of the crack. In the present investigation, the boundary collocation technique and the complex stress functions formulated are used to develop a new model of yielding at a crack tip. The new model assumes that the yield zone is circular instead of the wedge-shaped zone, thereby introducing a two-dimensional yield zone. Plastic zone lengths are calculated from the new model and are compared with those calculated from the Barenblatt-Dugdale model for the case of a crack in an infinite plate.

VI. SYMBOLS

A_n	nth coefficient in complex stress function
A_{sn}	nth coefficient for sth influence function
a	crack length, in.
B_n	nth coefficient in complex stress function
b	measurement of elliptical axis (major or minor) along the y axis, in.
C_n	nth coefficient in complex stress function
C_{jn}	nth coefficient for jth pole in complex stress function
c	distance from centerline of the crack to the back edge of the circular plastic zone, in.
D_n	nth coefficient in complex stress function
D_{jn}	nth coefficient for the jth pole in complex stress function
d	distance from centerline of the crack to the center of the circular hole, in.
e_m	error function at point m on the boundary
F	stress-intensity correction factor for the influence of a particular boundary condition
F_o	desired resultant force per unit thickness boundary condition in y direction, kips/in.
F_x	resultant force per unit thickness in x direction, kips/in.
F_y	resultant force per unit thickness in y direction, kips/in.
F_{sn}	nth coefficient for sth influence function
f	defined in equation (7)

G_o	desired resultant force per unit thickness boundary condition in x direction, kips/in.
G_{sn}	nth coefficient for sth influence function
g	defined in equation (7)
H_{sn}	nth coefficient for sth influence function
K_T	stress-concentration factor
k	stress-intensity factor, ksi-in$^{1/2}$
L_j	jth boundary
M	total number of points at which the error function was evaluated
M_O	resultant moment per unit thickness about origin, kips
N	number of coefficients in each series stress function
N_T	total number of coefficients used in the solution of a particular boundary-value problem
P	total resultant force per unit thickness acting on the boundary in x direction, kips/in.
p	pressure, ksi
Q	total resultant force per unit thickness acting on the boundary in y direction, kips/in.
R	measurement of elliptical axis (major or minor) along the x axis, in.
r	minimum radius of curvature for ellipse, in.
S	applied stress at infinity, ksi
u	displacement in x direction, in.
v	displacement in y direction, in.

x_j	coordinate location of pole on x axis, in.
y_j	coordinate location of pole on y axis, in.
z	complex variable, $z = x + iy$
z_j	location of pole in x,y plane
α	angle measured between the x axis and the normal to a boundary, radians
θ	angle measured between x axis and a line connecting the origin and a point on the boundary, radians
$\Delta\theta$	defined by equation (12)
ζ	coordinate measured along the contour of the boundary, in.
κ	material constant
Λ_j	contour around hole boundary L_j
λ	ratio of applied stress at infinity in the y direction to the stress in the x direction
μ	Lame's constant (shear modulus)
ν	Poisson's ratio
ρ	plastic zone length, in.
σ_o	yield stress for an elastic-perfectly plastic material, ksi
σ_x	internal stress in the x direction, ksi
σ_y	internal stress in the y direction, ksi
σ_n	applied stress normal to the boundary, ksi
τ_{nt}	applied shear stress tangential to the boundary, ksi
τ_{xy}	internal shear stress, ksi
$\Phi, \varphi, \psi, \Omega, \chi$	complex stress functions

VII. THEORETICAL DEVELOPMENTS

Complex Stress Functions For Cracked Bodies

One of the major developments in the field of two-dimensional elasticity has been the works of Muskhelishvili (ref. 8) on the complex potentials due to Kolosov for the two-dimensional equations of elasticity. The representation of biharmonic functions by analytic functions of the complex variable, $z = x + iy$, has led to a general method for solving plane strain and generalized plane stress problems. Further details on the Kolosov-Muskhelishvili method are given in appendix A.

The formulation of the complex potentials or stress functions for simply and multiconnected regions containing cracks follows that of Erdogan (ref. 13) and Kobayashi, Cherepy, and Kinsel (ref. 14).

In the sequel, it will be assumed that the configuration and loading are symmetric about the x and y axes. However, in the general case of nonsymmetrical loading and configuration, boundary-value problems can also be treated by the Kolosov-Muskhelishvili method.

Suppose we consider a straight crack which is located along the x axis as shown in figure 1. The complex stress functions for the configuration cut out by the dashed lines (annulus region) are given by

$$\left.\begin{aligned} \Phi(z) &= \Phi_0(z) + \Phi_1(z) \\ &\text{and} \\ \Psi(z) &= \Psi_0(z) + \Psi_1(z) \end{aligned}\right\} \tag{1}$$

The subscripts denote the corresponding stress functions which are used to approximate the boundary conditions on boundaries L_0 and L_1, respectively. The complex stress functions given in equation (1) are analytic inside the annulus region. The stress functions used to satisfy the boundary conditions on the external boundary L_0 are expressed as

$$\left.\begin{aligned} \Phi_0(z) &= \sqrt{z^2 - a^2} \sum_{n=0}^{\infty} A_n z^{2n} + z \sum_{n=0}^{\infty} B_n z^{2n} \\ &\text{and} \\ \Psi_0(z) &= \sqrt{z^2 - a^2} \sum_{n=0}^{\infty} A_n z^{2n} - z \sum_{n=0}^{\infty} B_n z^{2n} \end{aligned}\right\} \tag{2}$$

where the coefficients A_n and B_n are real. Further details on the formulation of these and other stress functions are given in appendix B. In the situation where the boundary L_0 is located at infinity, the coefficients A_0 and B_0 can be written in terms of the applied stress at infinity,

$$\left.\begin{aligned} A_0 &= \frac{S}{2} \\ &\text{and} \\ B_0 &= \frac{S}{4}(\lambda - 1) \end{aligned}\right\} \tag{3}$$

and the remaining coefficients are set equal to zero. For the internal boundary L_1, the stress functions are expressed as

$$\left.\begin{aligned}\Phi_1(z) &= \sqrt{z^2 - a^2}\sum_{n=1}^{\infty}\frac{C_n}{z^{2n}} + z\sum_{n=1}^{\infty}\frac{D_n}{z^{2n}}\\ \text{and}\qquad & \\ \psi_1(z) &= \sqrt{z^2 - a^2}\sum_{n=1}^{\infty}\frac{C_n}{z^{2n}} - z\sum_{n=1}^{\infty}\frac{D_n}{z^{2n}}\end{aligned}\right\}\tag{4}$$

where the coefficients C_n and D_n are real. These functions contain poles of various order at the origin and are used, primarily, to satisfy boundary conditions for cracks emanating from a circular hole. The stress functions, equations (2) and (4), automatically satisfy the boundary conditions on the crack surfaces. The conditions on the remaining boundaries are approximated by the series solution. The stress-intensity factor at the crack tip, $z = \pm a$, in figure 1 as calculated from equations (2) and (4) by using equation (31) and the relation $\varphi(z) = \Phi'(z)$ can be written as follows

$$k = S\sqrt{a}\left\{1 + \sum_{n=1}^{\infty} 2A_n a^{2n} + \sum_{n=1}^{\infty}\frac{2C_n}{a^{2n}}\right\}\tag{5}$$

where the term in the brackets is a dimensionless function which accounts for the influence of boundaries L_0 and L_1 on the stress-intensity factor for a single crack in an infinite plate.

In the special case of internal boundaries (multicircular or elliptical holes) which require the use of poles at various stations along the x or y axis, the stress functions are given by

$$\Phi_j(z) = \sqrt{z^2 - a^2} \sum_{n=1}^{\infty} \frac{C_{jn}}{(z^2 - z_j^2)^n} + z \sum_{n=1}^{\infty} \frac{D_{jn}}{(z^2 - z_j^2)^n}$$

and (6)

$$\Psi_j(z) = \sqrt{z^2 - a^2} \sum_{n=1}^{\infty} \frac{C_{jn}}{(z^2 - z_j^2)^n} - z \sum_{n=1}^{\infty} \frac{D_{jn}}{(z^2 - z_j^2)^n}$$

where the coefficients C_{jn} and D_{jn} are real. In these particular stress functions the pole, z_j, must lie on either the x or y axis and be symmetric about the y or x axis, respectively. These stress functions are used to satisfy the boundary conditions for a crack emanating from an elliptical hole and for the case of a crack in the presence of multiple-circular holes on the x or y axis. It should be noted that when the crack length approaches zero in these stress functions, they reduce to the form for multiply connected regions without cracks. For the general case where poles must be located off the axes, stress functions analogous to those in equation (6) may be generated to solve other types of boundary-value problems.

VIII. BOUNDARY COLLOCATION METHOD

The method of boundary collocation is a numerical technique used for obtaining solutions to various types of boundary-value problems. The technique begins with an exact series solution to a given linear partial differential equation which contains a specified number of unknown coefficients. The conditions of symmetry can be used to eliminate those terms in the series which are inappropriate for the problem being investigated. In the case of two-dimensional elasticity problems the biharmonic equation is the governing partial differential equation for the region of interest. The values of the unknown coefficients are then determined from linear simultaneous equations that satisfy certain specified conditions on the boundaries; such as stress, force, or displacement. The series solution obtained satisfies the prescribed conditions in the interior of the region exactly, and those on the boundary approximately.

Various techniques have been used by several investigators to satisfy the conditions along the boundary of simply and multiconnected regions. In a technique used by Conway (ref. 15), the values of the coefficients were determined from the criterion that the boundary conditions should be satisfied exactly at a specified number of evenly spaced points along the boundary. Hulbert, et al. (ref. 16) and Hooke (ref. 17) used the criterion that the coefficients should be selected so that the sum of the squares of the stress residuals at a specified number of points on the boundary should be a minimum. Kobayashi, Cherepy, and Kinsel (ref. 14) used the former technique and

Hulbert, et al. (ref. 16) used the latter technique for analyzing a finite plate with a crack. The techniques employed in the present investigation consist of specifying the stresses at equally spaced points on the boundary, specifying the resultant forces along arcs on the boundary, and a least-squares technique used for minimizing the resultant force or displacement residuals along the boundary. The three techniques were used in the solution of several boundary-value problems in order to compare their rates of convergence. Further details on the technique used for specifying the boundary stresses are given in appendix C. The techniques treated herein concern the methods used for specifying the resultant forces or displacements on the boundary and that used for minimizing the resultant force or displacement residuals along the boundary.

The complex equation for the resultant forces and displacements, see appendix A, can be written in terms of Φ and ψ as

$$\beta\Phi(z) + \psi(\overline{z}) + (z - \overline{z})\overline{\Phi'(z)} = f + ig \tag{7}$$

where

$$\beta = 1 \qquad f = -F_y\Big|_{\zeta_0}^{\zeta} \qquad g = F_x\Big|_{\zeta_0}^{\zeta}$$

$$\beta = -\kappa \qquad f = -2\mu u \qquad g = -2\mu v$$

The location of ζ_0 is completely arbitrary, however, for all problems considered the location was the intersection of the boundary with the x or y axis. Further details on the location of ζ_0 are given in the section on the "Application of the Boundary Collocation Method." From the complex stress functions Φ and ψ (for example, eq. (2)) the expression for f and g can be written as

$$\left.\begin{aligned} f &= \sum_{n=0}^{N} A_n F_{1n}\Big|_{\zeta_0}^{\zeta} + \sum_{n=0}^{N} B_n F_{2n}\Big|_{\zeta_0}^{\zeta} \\ g &= \sum_{n=0}^{N} A_n G_{1n}\Big|_{\zeta_0}^{\zeta} + \sum_{n=0}^{N} B_n G_{2n}\Big|_{\zeta_0}^{\zeta} \end{aligned}\right\} \tag{8}$$

where F_{sn} and G_{sn} $(s = 1,2)$ denote the influence functions for the respective unknown coefficients. In the case of multiple boundaries or poles the contribution to f and g due to each additional stress function must be added to equations (8). It should be noticed that in equations (8), the number of terms in each series are truncated to the same number of coefficients. This was found to be a computational advantage in formulating the matrix solution. The values of the functions F_{sn} and G_{sn} at the lower limit ζ_0 were determined from the location of ζ_0 in the various stress boundary-value problems. For displacement boundary-value problems, the values of F_{sn} and G_{sn} at the lower limit must be set equal to zero, see equation (7). The values of A_0 and B_0 were determined from the stress conditions at infinity for the case of a crack in an infinite plate. The conditions along the various boundaries were specified for the particular boundary-value problem considered.

In the technique used for specifying the resultant forces along arcs on the boundary, equations (8) were evaluated at N points on the boundary and the resulting equations were solved on a computer for the unknown coefficients. Further details on the computer and matrix solutions are given in the section on "Digital Computer and Matrix Solution." The resulting coefficients were then used to calculate the stress-intensity factor and the local stress distributions from the appropriate stress functions.

In general, there will be an error in the boundary condition at a given point m, since there are only a finite number of unknown coefficients in equations (8), and the square of this error is written as

$$e_m^2 = \left\{F_0 - \sum_{n=0}^{N} A_n F_{1n}\Big|_{\zeta_0}^{\zeta} - \sum_{n=0}^{N} B_n F_{2n}\Big|_{\zeta_0}^{\zeta}\right\}_m^2 + \left\{G_0 - \sum_{n=0}^{N} A_n G_{1n}\Big|_{\zeta_0}^{\zeta} - \sum_{n=0}^{N} B_n G_{2n}\Big|_{\zeta_0}^{\zeta}\right\}_m^2 \tag{9}$$

where F_0 and G_0 are the desired boundary conditions and F_{sn} and G_{sn} are the influence functions from equations (8) evaluated at point m. In the case of multiple boundaries or poles the contribution of additional stress functions to the error at point m must be added to each term in equation (9). If the criterion is used that the sum of the squares of the errors at a specified number of points, M, along the boundary should be a minimum,

$$\frac{\partial \sum_{m=1}^{M} e_m^2}{\partial A_p} = 0 \qquad \frac{\partial \sum_{m=1}^{M} e_m^2}{\partial B_p} = 0 \tag{10}$$

a set of symmetrical simultaneous equations for the coefficients A_n and B_n are obtained

$$\left.\begin{aligned}
&\sum_{p=1}^{N} \alpha_{np}A_n + \sum_{p=1}^{N} \beta_{np}B_n = \Delta_p \\
&\sum_{p=1}^{N} \beta_{pn}A_n + \sum_{p=1}^{N} \gamma_{np}B_n = \epsilon_p \\
&\text{where} \\
&\alpha_{np} = \sum_{m=1}^{M} (F_{1n}F_{1p} + G_{1n}G_{1p}) \\
&\beta_{np} = \sum_{m=1}^{M} (F_{2n}F_{1p} + G_{2n}G_{1p}) \\
&\gamma_{np} = \sum_{m=1}^{M} (F_{2n}F_{2p} + G_{2n}G_{2p}) \\
&\Delta_p = \sum_{m=1}^{M} (F_0F_{1p} + G_0G_{1p}) \\
&\text{and} \\
&\epsilon_p = \sum_{m=1}^{M} (F_0F_{2p} + G_0G_{2p})
\end{aligned}\right\} \tag{11}$$

The second partial of the error function with respect to the unknown coefficients is positive indicating a definite minimum. These equations were solved on the computer and the resulting coefficients were resubstituted into the appropriate stress function to calculate the stress-intensity factor and the local stress distributions.

In the least-squares boundary collocation method, previously described, it was necessary to specify the points on the boundary at which the error function, equation (9), was evaluated. The procedure used to specify these locations on the circular and elliptic boundaries was to vary in equal increments the angle θ, see figure 2. The values of r, R, and b are the radius of curvature (defined in fig. 2), major axis and minor axis for the elliptical hole, respectively. The increment, $\Delta\theta$, is determined by

$$\Delta\theta = \frac{\theta_o}{M} \qquad (12)$$

where M is the total number of points on the boundary at which the error function is evaluated. This procedure automatically concentrates more points along the sections of the boundary which have smaller radii of curvature. In general, the value of M used in the solution of the boundary-value problems in the section "Application of the Boundary Collocation Method" was twice the total number of unknown coefficients in the stress functions.

IX. APPLICATION OF THE BOUNDARY COLLOCATION METHOD

In the following section the boundary collocation method and the complex variable method of Muskhelishvili were used to analyze various boundary-value problems. The types of configurations considered can be grouped into three categories: (1) cracks emanating from a circular hole, (2) cracks in the vicinity of multiple-circular holes, and (3) cracks emanating from an elliptical hole in an infinite plate. In each category a variety of boundary conditions were investigated. The least-squares technique, as previously discussed, was used to satisfy the boundary conditions in the final analysis of each boundary-value problem. The number of unknown coefficients used in the complex stress function (eq. (41)) was 90 for the circular holes and 160 for the elliptical hole. The results are presented in terms of a crack tip stress-intensity correction factor which accounts for the influence of the various boundaries on the stress-intensity factor for a single crack in an infinite plate.

Circular Hole

For the case of cracks emanating from a circular hole, figure 3, several collocation techniques were used to satisfy the conditions on the circular boundary. The results of these techniques are compared in figure 4 and included such techniques as specifying the stresses at equally spaced points on the boundary, specifying the resultant forces along arcs on the boundary and the least-squares technique used for minimizing the resultant force residuals along the boundary. In the force equations (eq. (7)), the location of the lower limit ζ_0 was the intersection of the hole boundary with the x axis in the first quadrant. In all of the techniques used the complex stress function had a pole at the origin, $z_j = 0$. The analysis using the least-squares technique was found to converge considerably faster than the other two methods. The complex stress functions, equations (36) and (41), were both used in the comparison of convergence in the case of the technique using resultant forces. In specifying stresses at points, the convergence curve is only shown for equation (36). In the least-squares technique two convergence curves are presented, one for the situation where the number of points, M, considered on the boundary was equal to the total number of coefficients in the stress functions and the other was for the case where the number of points considered was five times the number of coefficients. All techniques were found to converge as the number of coefficients increased.

The correction factors for cracks growing from a circular hole subjected to a remote stress at infinity were originally solved by Bowie (ref. 4), using a conformal mapping procedure; however, the values given in figure 5 (open circles) were obtained from a table listed in reference 18. The solid curves in figure 5 show the results obtained in the present investigation for three states of remote stress. The overall agreement with Bowie's solutions was considered good.

In a similar configuration to that above, internal pressure was applied to both the circular and crack boundaries as shown in figure 6. The correction factors for two values of pressure applied on the crack surfaces are shown in figure 7. In the situation where no pressure is applied to the crack surfaces ($\lambda = 0$), the correction factor approaches zero as the crack length approaches infinity. The dashed curve shows the stress-intensity solution for the case of wedge-force loading on the crack surfaces expressed in terms of the correction factor, F. The wedge-force equation (ref. 18) is given as

$$k = \frac{P}{\pi \sqrt{a}} = \frac{2Rp}{\pi \sqrt{a}} \tag{13}$$

where the value of P is the resultant force per unit thickness acting in the y direction due to the internal pressure, p. The solid and dashed curves converge as the crack length increases. In the case where $\lambda = 1$ the correction factor approaches unity, as would be expected.

As previously mentioned, Vitvitski and Leonov (ref. 12) presented the solution for the Barenblatt-Dugdale model for a circular hole in an infinite plate subjected to a uniaxial remote stress, see figure 8. In the present investigation the correction factors given in figures 5 and 7 were used to derive the solution for the Barenblatt-Dugdale model for the circular hole subjected to three separate states of remote stress. The plastic zone lengths calculated are shown in figure 9 as a function of the ratio of applied stress to that of the yield stress of the material. The solid circles plotted in figure 9 show the plastic zone lengths calculated by Vitvitski and Leonov; and these values were obtained from a table given in reference 19. The agreement between the solid circles and the present solution is good at the lower values of applied stress; however, at the larger values the disagreement is considerable. At the larger values of applied stress, the plastic zone calculations in the present solution approach the Barenblatt-Dugdale model, indicating that the circular hole had a negligible effect on the crack tip stress-intensity factor for large values of plastic zone length.

For the case of a biaxial stress at infinity ($\lambda = 1$), Savin (ref. 20) presented a closed form solution for the plastic zone size and the results are shown in figure 9 as the dashed curve. The analysis given by Savin assumes that the plastic zone is a concentric circle around the circular hole. The disagreement between the solid and dashed curves for $\lambda = 1$ is expected, primarily, because of the differences in the assumed plastic zone configurations.

Multiple-Circular Holes

In the case of a multiconnected region as shown in figure 10, the complex stress function (eq. (41)) was used with poles located at $z_j = \pm d$. The location of the lower limit ζ_0 used in the force equations (eq. (7)) was the intersection of the hole boundary with the x axis at $x = R + d$. The correction factors for the case of a crack approaching two circular holes in an infinite plate subjected to a uniaxial state of stress are shown in figure 11 for several values of d/R. The correction factors are plotted against the ratio of crack length, a, to the net section between the two holes, $d - R$. The correction factors increase from their initial values at $a = 0$ to extremely high values as the crack length approaches the edge of the hole. The correction factors are elevated at small values of crack length because of the increase in the local stresses between the two holes.

In the maintenance of aircraft structures the growth of fatigue cracks is very commonly delayed or stopped by drilling holes at the ends of the crack to eliminate the high stress concentrations. The resulting boundary-value problem is similar to the configuration previously shown, see figure 10, and corresponds to the case where the crack intersects the two circular holes ($a = d$). The stress concentration factor at the edge of the hole ($x = R + d$) was calculated as a function of the ratio of hole radius, R, to the pole location, d, see figure 12. The stress concentration factors were compared with those calculated from the elliptical hole solution as shown by the dashed line. The elliptical hole had the same radius of curvature as the circular holes and their overall lengths were equivalent. The stress concentration factor for the elliptical hole was consistently lower than those for the case of two circular holes connected by a crack or slit.

As previously mentioned, Barenblatt and Dugdale have developed a simple model of yielding at the tip of a crack. The plastic zone is assumed to be an extension of the crack with surface tractions applied along the extension to simulate the plastic behavior. In the present investigation, a new model of yielding at the crack tip under extensional loading is developed. The new model assumes that the yield zone is circular, thereby introducing a two-dimensional yield zone, see figure 13. As a matter of interest, the plastic zone size at a crack tip subjected to longitudinal shear is circular, see reference 21.

The plastic material (shaded region) is assumed to carry load only in the y direction and the stress component on the circular boundary is set equal to the yield stress of the material. The criterion used to calculate the plastic zone size, ρ, is that the local stress at the front edge of the circular zone ($x = c + \rho$) is equal to the yield stress of the material. This criterion is similar to that used by Barenblatt and Dugdale. In figure 14, the plastic zone lengths calculated from the new model are compared with those calculated from the Barenblatt-Dugdale model for a crack in an infinite plate. The equation for the Barenblatt-Dugdale model is

$$\rho = c \left\{ \sec \frac{\pi S}{2\sigma_o} - 1 \right\} \tag{14}$$

The results based on the new model show a considerable reduction in the plastic zone length from those calculated by the Barenblatt-Dugdale model for low values of applied stress. In actuality, the plastic zone is neither circular nor wedge shaped, as in the Barenblatt-Dugdale model, but takes a similar shape to that of a "butterfly wing," see reference 22.

A further example of a multiconnected region containing cracks is that of a crack located between two circular holes where the centerline of the holes is perpendicular to the plane of the crack, see figure 15. The correction factors for this case are shown in figure 16 for several values of d/R. An interesting observation from the stress-intensity solution is that the value of the correction factor, F, is equivalent in magnitude to the local stress concentration factor at the origin as the crack length approaches zero. The stress-intensity factor at the crack tip as the crack length approaches zero can be written in terms of the local stress at the origin and the remote stress as follows

$$k = \sigma_y \sqrt{a} = S \sqrt{a}\, F \tag{15}$$

where σ_y is the local stress at the origin for the case of an infinite plate with two circular holes. From equation (15), the relation between the local stress and the correction factor is

$$F = \frac{\sigma_y}{S} = K_T \tag{16}$$

The local stress concentration at the origin for the case of two circular holes in an infinite plate with no crack was obtained from reference 20 for a value of $d/R = 2$ and is plotted as the open circle on the ordinate axis.

Elliptical Hole

For the case of cracks emanating from an elliptical hole, figure 17, the complex stress functions, equations (36) and (41), contained multiple poles located either on the x or y axis. The poles were always located along the major axis of the ellipse. These poles were equally spaced between and located at the origin and the center of the minimum radius of curvature. In order to show convergence, both collocation techniques employing the force equations were used to satisfy the conditions on the elliptic boundary. The results of these techniques are shown in figure 18. The ratio of the minor to the major axis was 0.25 and the ratio of crack length to the major axis was 1.01. The major axis was located along the x axis, see figure 17. In the specification of resultant forces along arcs on the boundary, equations (36) and (41) were both used with 16 poles located on the x axis in the first quadrant. In the least-squares technique used to minimize the resultant force residuals, there were also 16 poles located on the x axis. The least-squares technique was found to converge considerably faster than the technique using only resultant forces.

The correction factors for cracks growing from an elliptical hole subjected to a uniaxial stress at infinity are shown in figure 19 for several values of b/R. However, only two ratios of major to minor axis were considered and they were 2 to 1 and 4 to 1. The number of poles used in equation (41) for the 2 to 1 and 4 to 1 ellipse were 4 and 16, respectively. The dashed curves show the theoretical limits expressed in terms of the correction factor, F, as the value of b approaches either zero or infinity. The crack tip stress-intensity factor in the limiting case, $b = \infty$, was obtained from the edge crack solution (ref. 18) and is written as

$$k = 1.12\, S\sqrt{a - R} \tag{17}$$

The other limit is for the case where the elliptical hole reduces to a crack or slit. In all cases, except the edge crack solution, the value of the correction factor approaches unity as the crack length approaches infinity. The edge crack solution approaches 1.12.

X. DIGITAL COMPUTER AND MATRIX SOLUTION

The computer system which was used to solve the linear simultaneous equations and make the necessary calculations was a Control Data Corporation 6000 Series Digital Computer using single precision (14 digits). The linear simultaneous equations were solved by a subroutine called from storage in the Langley Research Center computer complex which employed Jordan's method (ref. 23) to solve for the unknown coefficients. The computer calculations required from 1 to 4 minutes of computer time to solve 90 to 180 equations, respectively, and to furnish the necessary output.

XI. CONCLUDING REMARKS

Stress-intensity factors have been presented for several boundary-value problems involving cracks in the presence of stress concentrations. The types of configurations investigated included the case of crack emanating from a circular hole, the case of a crack in the presence of multiple-circular holes, and the case of cracks emanating from an elliptical hole in an infinite plate subjected to a variety of loading conditions. The solution of these problems was based on the complex variable method of Muskhelishvili and a numerical technique referred to as boundary collocation. The complex stress functions developed automatically to satisfy the boundary conditions on the crack surfaces. The conditions on the remaining boundaries were approximated by the series solution. In general, the least-squares technique used for minimizing the resultant force residuals along the boundary gave better convergence in the boundary conditions than the techniques employing only the resultant force or stress equations.

XII. APPENDIX A

KOLOSOV-MUSKHELISHVILI METHOD

In the following section, the basic equations of the Kolosov-Muskhelishvili method (ref. 8) are given and the series stress functions for simply and multiply connected regions are formulated.

Suppose we consider a region, figure 20, simply or multiply connected, on the x,y plane bounded by a number of contours, L_j. The interior of the region is considered to represent a disk of unit thickness. The known surface tractions are to be applied on the boundaries of this region. The body forces are assumed to be zero and the material is assumed to be isotropic and homogeneous. The equilibrium and compatibility equations for this region can be combined to form the biharmonic equation

$$\frac{\partial^4 U}{\partial x^4} + 2\frac{\partial^4 U}{\partial x^2 \partial y^2} + \frac{\partial^4 U}{\partial y^4} = 0 \tag{18}$$

where $U(x,y)$ is the Airy stress function. It is a well-known fact that the biharmonic function $U(x,y)$ can be expressed as

$$U(x,y) = \mathrm{Re}\left[\bar{z}\Phi(z) + X(z)\right] \tag{19}$$

where $\Phi(z)$ and $X(z)$ are two analytic functions. Therefore, the generalized plane stress and plane strain problems of elasticity are reduced to the determination of these functions from the specified boundary conditions. For this purpose, we must express the boundary conditions in terms of $\Phi(z)$ and $X(z)$.

In the case of the first fundamental problem of elasticity the complex equation for the normal and tangential shear stress applied to the boundary can be expressed in terms of the redefined stress functions $(\varphi(z),\ \Omega(z))$ as

$$\sigma_n - i\tau_{nt} = \varphi(z) + \overline{\varphi(z)} - \left[(\overline{z} - z)\varphi'(z) - \varphi(z) + \overline{\Omega}(z)\right]e^{2i\alpha} \tag{20}$$

where

$$\varphi(z) = \Phi'(z)$$

and

$$\Omega(z) = \overline{\Phi}'(z) + z\overline{\Phi}''(z) + \overline{X}''(z) = \psi'(z)$$

The stresses at an interior point z are given by

$$\left.\begin{aligned} \sigma_x + \sigma_y &= 2\left[\varphi(z) + \overline{\varphi(z)}\right] \\ \sigma_y - \sigma_x + 2i\tau_{xy} &= 2\left[(\overline{z} - z)\varphi'(z) - \varphi(z) + \overline{\Omega}(z)\right] \end{aligned}\right\} \tag{21}$$

In the case of the second fundamental problem, the displacements at a point are given by

$$2\mu(u + iv) = \kappa \int_0^z \varphi(z)dz - \int_0^{\overline{z}} \Omega(\overline{z})d\overline{z} - (z - \overline{z})\overline{\varphi(z)} \tag{22}$$

where $\kappa = 3 - 4\nu$ for the case of plane strain,

$$\kappa = \frac{3 - \nu}{1 + \nu}$$

for the case of plane stress, ν and μ are Poisson's ratio and Lame's constant, respectively.

In addition, we have the following expressions for the resultant forces, F_x and F_y, and the moment, M_o, about the origin due to the surface tractions acting on the arc $\zeta_0 - \zeta$ on the boundary.

$$\left.\begin{aligned}
F_x + iF_y &= -i\left[\int \varphi(z)dz + \int \Omega(\overline{z})d\overline{z} + (z - \overline{z})\overline{\varphi(z)}\right]\Bigg|_{\zeta_0}^{\zeta} \\
M_o &= \mathrm{Re}\left[\int\int \left[\varphi(z) + \overline{\Omega}(z)\right]dzdz - z\int\left[\varphi(z) + \overline{\Omega}(z)\right]dz + z(z - \overline{z})\varphi(z)\right]\Bigg|_{\zeta_0}^{\zeta}
\end{aligned}\right\} \quad (23)$$

If the complex functions on the right-hand side of equations (20) to (23) are known, a separation into real and imaginary parts will determine the components on the left-hand side.

For the particular case of an infinite plate with a single hole with the origin of the coordinate system located inside the hole, the stress functions $\varphi(z)$ and $\Omega(z)$ outside the boundary of the hole can be written as

$$\left.\begin{aligned}
\varphi(z) &= \sum_{n=-\infty}^{\infty} A_n' z^n \\
\Omega(z) &= \sum^{\infty} B_n' z^n
\end{aligned}\right\} \quad (24)$$

In these equations the coefficients A'_{-1} and B'_{-1} are not independent but are related by

$$B'_{-1} = -\kappa A'_{-1} = \frac{\kappa(P - iQ)}{2\pi(1 + \kappa)} \tag{25}$$

The values of P and Q are the total resultant forces per unit thickness exerted on the contour of the hole. If no resultant forces are applied to the hole boundary the magnitude of P and Q is zero. If the stress components at infinity are to remain finite, the coefficients A'_n and B'_n in the stress functions must be zero for $n \geq 1$. Therefore, the functions will be of the type

$$\left.\begin{aligned} \varphi(z) &= A'_0 + \varphi_1(z) \\ \Omega(z) &= B'_0 + \Omega_1(z) \end{aligned}\right\} \tag{26}$$

where the complex coefficients A'_0 and B'_0 can be written in terms of the applied stress at infinity. The functions $\varphi_1(z)$ and $\Omega_1(z)$ are holomorphic outside the hole boundary and including the point at infinity. Therefore, for sufficiently large $|z|$ they may be expanded in a series of the form

$$\left.\begin{aligned} \varphi_1(z) &= \frac{A'_{-2}}{z^2} + \frac{A'_{-3}}{z^3} + \frac{A'_{-4}}{z^4} + \dots \\ \Omega_1(z) &= \frac{B'_{-2}}{z^2} + \frac{B'_{-3}}{z^3} + \frac{B'_{-4}}{z^4} + \dots \end{aligned}\right\} \tag{27}$$

For the case where the single hole is circular and loading is either uniform stress at infinity or uniform stress around the boundary of the hole, the exact solution can be written from a finite number of terms in equation (27).

In the general case, as in figure 20, for a multiply connected region the formulation of the complex stress functions are more complicated and are given by

$$\left.\begin{aligned} \varphi(z) &= \sum_{n=0}^{\infty} A_n' z^n + \sum_{j=1}^{J} \sum_{n=1}^{\infty} \frac{A_{jn}'}{(z - z_j)^n} \\ \Omega(z) &= \sum_{n=0}^{\infty} B_n' z^n + \sum_{j=1}^{J} \sum_{n=1}^{\infty} \frac{B_{jn}'}{(z - z_j)^n} \end{aligned}\right\} \qquad (28)$$

where z_j lies inside the internal boundary, L_j. In these equations the coefficients A_{j1}' and B_{j1}' are not independent but are related by equation (25). These stress functions are used to satisfy the boundary conditions for regions which contain no singularities on the hole boundary.

XIII. APPENDIX B

FORMULATION OF THE COMPLEX STRESS FUNCTIONS FOR CRACKED BODIES

The theoretical formulation of the stress functions for two-dimensional cracked bodies follows that of Erdogan (ref. 13), which was based on Muskhelishvili's method (ref. 8) for an infinite plate, isotropic and homogeneous, containing cracks and subjected to inplane loading. From reference 8 it is seen that at the crack tip $(z = a)$ the functions $\varphi(z)$ and $\Omega(z)$ can be written as,

$$\left.\begin{aligned} \varphi(z) &= \frac{H_1(z)}{\sqrt{z - a}} + H_2(z) \\ \Omega(z) &= \frac{H_1(z)}{\sqrt{z - a}} + H_3(z) \end{aligned}\right\} \tag{29}$$

where $H_s(z)$ are holomorphic and can be expressed as

$$H_s(z) = \sum_{n=0}^{\infty} A'_{sn}(z - a)^n \tag{30}$$

The strength of the singularity at the crack tip is characterized in what is referred to as the stress-intensity factor. The stress-intensity factor is determined by

$$k = 2\sqrt{2} \lim_{z \to a} \sqrt{z - a}\, \varphi(z) \tag{31}$$

In the sequel, the formulation of the complex stress functions for simply and multiply connected regions containing cracks is restricted to the situation where the configuration and loading are symmetric about the x and y axes. The boundary conditions that must be satisfied by φ and Ω are given as follows

$$\left.\begin{array}{llll} \text{(I)} & \sigma_y = \tau_{xy} = 0 & |x| < a & y = 0 \\ \text{(II)} & \tau_{xy} = v = 0 & |x| \geq a & y = 0 \\ \text{(III)} & \tau_{xy} = u = 0 & |y| \geq 0 & x = 0 \end{array}\right\} \qquad (32)$$

where the coordinate system used is shown in figure 21. The notations x_j and y_j denote the location of poles on the x and y axes, respectively.

The boundary conditions stated in equation (32) are sufficient to define a relationship between the two analytic functions φ and Ω. The relationship for the term which contains the square root singularity is $\varphi(z) = \Omega(z)$ and for the term which contains no square root singularity is $\varphi(z) = -\Omega(z)$. For the special case of symmetric loading about the x axis on the crack surfaces, the relationship between the two analytic functions is $\varphi(z) = \Omega(z)$.

In addition to the boundary conditions stated in equation (32), the condition which requires the single valuedness of displacements in a multiply connected domain must also be satisfied. This condition can be stated as

$$\kappa \oint_{\Lambda_j} \varphi(z)dz - \oint_{\Lambda_j} \Omega(\overline{z})d\overline{z} = 0 \qquad (33)$$

where Λ_j is the contour around each separate hole boundary, L_j.

The formulation of the stress functions for the external and the internal boundaries will be treated separately. For the external boundary which is symmetric about the x and y axes, the stress function can be written as

$$\varphi_0(z) = \frac{z}{\sqrt{z^2 - a^2}} \sum_{n=0}^{\infty} A_n' z^{2n} + \sum_{n=0}^{\infty} B_n' z^{2n} \qquad (34)$$

where A_n' and B_n' are real coefficients. This function is similar to the function used by Kobayashi, Cherepy, and Kinsel (ref. 14) for the case of a crack in a finite plate. In order to use this function in the least-squares boundary collocation method employing force equations, it is convenient to express φ_0 in terms of Φ_0, where $\Phi_0'(z) = \varphi_0(z)$. The redefined stress function is obtained by integrating equation (34) and is given by

$$\Phi_0(z) = \sqrt{z^2 - a^2} \sum_{n=0}^{\infty} A_n z^{2n} + z \sum_{n=0}^{\infty} B_n z^{2n} \qquad (35)$$

where A_n and B_n are redefined coefficients. This function is identical to the function used by Hulbert, et al. (ref. 16), for the case of a crack in a finite plate.

For the case of internal boundaries which are symmetric about the x and y axis, the stress function can be expressed as

$$\varphi_j(z) = \frac{z}{\sqrt{z^2 - a^2}} \sum_{n=1}^{\infty} \frac{C'_{jn}}{(z^2 - z_j^2)^n} + \sum_{n=1}^{\infty} \frac{D'_{jn}}{(z^2 - z_j^2)^n} \tag{36}$$

where C'_{jn} and D'_{jn} are real coefficients. The pole z_j must be located either on the x or y axis as shown in figure 21. Again it is convenient to express φ_j in terms of Φ_j, as previously defined. However, for the situation where the poles are located on the x axis, the integral of equation (36) depends upon the relative magnitude of x_j. Therefore, it is of interest to investigate the four possible locations of the pole, x_j. Reference 24 was used to evaluate some of the more difficult integrals.

<u>Case I</u>: $z_j = x_j = 0$

$$\Phi_j(z) = C_{j1}\left[-\frac{1}{a}\tan^{-1}\left(\frac{a}{\sqrt{z^2 - a^2}}\right)\right] + \sum_{n=2}^{\infty} C_{jn} \frac{\sqrt{z^2 - a^2}}{z^{2n-2}} + \sum_{n=2}^{\infty} \frac{D_{jn}}{z^{2n-3}} \tag{37}$$

Case II: $|z_j| = |x_j| < a$

$$\Phi_j(z) = C_{j1}\left[\frac{-1}{\sqrt{a^2 - x_j^2}} \tan^{-1}\sqrt{\frac{a^2 - x_j^2}{z^2 - a^2}}\right] + \sum_{n=2}^{\infty} C_{jn} \frac{\sqrt{z^2 - a^2}}{(z^2 - x_j^2)^{n-1}}$$

$$+ D_{j1}\left[\frac{1}{2x_j} \ln\left(\frac{z - x_j}{z + x_j}\right)\right] + \sum_{n=2}^{\infty} D_{jn} \frac{z}{(z^2 - x_j^2)^{n-1}} \tag{38}$$

Case III: $z_j = x_j = a$

$$\Phi_j(z) = \sum_{n=2}^{\infty} C_{jn} \frac{\sqrt{z^2 - a^2}}{(z^2 - x_j^2)^{n-1}} + D_{j1}\left[\frac{1}{2x_j} \ln\left(\frac{z - x_j}{z + x_j}\right)\right]$$

$$+ \sum_{n=2}^{\infty} D_{jn} \frac{z}{(z^2 - x_j^2)^{n-1}} \qquad (39)$$

Case IV: $z_j = x_j > a$

$$\Phi_j(z) = C_{j1}\left[\frac{1}{2\sqrt{x_j^2 - a^2}} \ln\left(\frac{\sqrt{z^2 - a^2} - \sqrt{x_j^2 - a^2}}{\sqrt{z^2 - a^2} + \sqrt{x_j^2 - a^2}}\right)\right] + \sum_{n=2}^{\infty} C_{jn} \frac{\sqrt{z^2 - a^2}}{(z^2 - x_j^2)^{n-1}}$$

$$+ D_{j1}\left[\frac{1}{2x_j} \ln\left(\frac{z - x_j}{z + x_j}\right)\right] + \sum_{n=2}^{\infty} D_{jn} \frac{z}{(z^2 - x_j^2)^{n-1}} \qquad (40)$$

In equations (37) through (40), the coefficients C_{jn} and D_{jn} are redefined coefficients. In equation (40), it is necessary to set $C_{j1} = D_{j1} = 0$ to satisfy the displacement conditions along the x axis between the crack tip and the location of the pole.

In order to obtain a general stress function which can be used for all possible locations of the poles on the x or y axis, the coefficients C_{j1} and D_{j1} are arbitrarily set equal to zero in equations (37) through (40). The resulting stress function is

$$\Phi_j(z) = \sum_{n=2}^{\infty} C_{jn} \frac{\sqrt{z^2 - a^2}}{(z^2 - z_j^2)^{n-1}} + \sum_{n=2}^{\infty} D_{jn} \frac{z}{(z^2 - z_j^2)^{n-1}} \qquad (41)$$

This stress function was used for the case of poles located on and symmetric about the x or y axis. In the application of the boundary collocation method, equations (36) and (41) were both used in the solution of a few selected boundary-value problems in order to compare their individual convergence. This stress function was also used to analyze various notch problems by setting the crack length equal to zero.

XIV. APPENDIX C

STRESS CONDITIONS ON THE CIRCULAR BOUNDARY

The boundary collocation technique treated herein concerns the method used to specify the normal stress and tangential shear stress components on a circular boundary. The case investigated had two cracks emanating from a circular hole in an infinite plate. The complex equation for the two stress components on the boundary can be written as

$$\sigma_n - i\tau_{nt} = \varphi(z) + \overline{\varphi(z)} - \left[(\overline{z} - z)\varphi'(z) - \varphi(z) + \overline{\Omega}(z)\right]e^{2i\theta} \tag{42}$$

where

$$\varphi(z) = \frac{z}{\sqrt{z^2 - a^2}} \sum_{n=1}^{N} \frac{C_n'}{z^{2n}} + \sum_{n=1}^{N} \frac{D_n'}{z^{2n}} + \varphi_0(z) \tag{43}$$

and

$$\Omega(z) = \frac{z}{\sqrt{z^2 - a^2}} \sum_{n=1}^{N} \frac{C_n'}{z^{2n}} - \sum_{n=1}^{N} \frac{D_n'}{z^{2n}} + \Omega_0(z) \tag{44}$$

The stress functions φ_0 and Ω_0 were determined from the desired stress conditions either on the crack surfaces or at infinity for a single crack in an infinite plate. The remaining coefficients were determined from the conditions that $\sigma_n = 0$ and $\tau_{nt} = 0$ at equally spaced points on the circular boundary, see figure 22. The resulting simultaneous equations were solved on the computer using single precision. The equation for the stress-intensity factor for the configuration shown in figure 22 as calculated by equation (31) is as follows

$$k = S\sqrt{a}\left[1 + \sum_{n=1}^{N} \frac{2C_n'}{a^{2n}}\right] \tag{45}$$

where the term in the brackets is the correction factor for the influence of the circular hole on the stress-intensity factor for a single crack in an infinite plate.

XV. REFERENCES

1. Paris, P. C., Gomez, M. D., and Anderson, W. E., "A Rational Analytic Theory of Fatigue," The Trend in Engineering, University of Washington, Vol. 13, No. 1, January 1961.

2. Donaldson, D. R., and Anderson, W. E., "Crack Propagation Behavior of Some Air Frame Materials," Crack Propagation Symposium, The College of Aeronautics, Cranfield, England, 1961.

3. Figge, I. E., and Newman, J. C., Jr., "Prediction of Fatigue-Crack-Propagation Behavior in Panels With Simulated Rivet Forces," NASA TN D-4702, 1968.

4. Bowie, O. L., "Analysis of an Infinite Plate Containing Radial Cracks Originating From a Circular Hole," Journal of Math and Phys., Vol. 23, No. 1, 1956.

5. Grebenkin, G. G., and Kaminskii, A. A., "Propagation of Cracks Near an Arbitrary Curvilinear Hole," Fiziko-Khimicheskaya Mekhanika Materialov, Vol. 3, No. 4, 1967.

6. Erdogan, F., "Elastic-Plastic Anti-Plane Problems in Infinite Planes and Strips With Cracks or Cavities, NASA Contract NGR 39-007-011, Lehigh University, 1966.

7. Isida, M., "Crack Tip Stress Intensity Factors For a Crack Approaching a Hole Centered on Its Plane," Lehigh University, 1966.

8. Muskhelishvili, N. I., Some Basic Problems of Mathematical Theory of Elasticity, P. Noordhoff, 1953.

9. Hulbert, L. E., The Numerical Solution of Two-Dimensional Problems of the Theory of Elasticity, Bulletin 198, Engineering Experiment Station, Ohio State University.

10. Barenblatt, G. I., "Mathematical Theory of Equilibrium Cracks in Brittle Fracture," Advances in Applied Mechanics, Vol. VII, Academic Press, 1962.

11. Dugdale, D. S., "Yielding of Steel Sheets Containing Slits," Jour. Mech. Phys. Solids, Vol. 8, 1960.

12. Vitvitski, P. M., and Leonov, M. Y., "Slip Bands at Nonuniform Deformation of a Plate," VMRTT, Izdat, USSR, No. 1, Keiv, 1962.

13. Erdogan, F., "On the Stress Distribution in Plates With Collinear Cuts Under Arbitrary Loads," Proceedings Fourth U.S. National Congress of Applied Mechanics, 1962.

14. Kobayashi, A. S., Cherepy, R. D., and Kinsel, W. C., "A Numerical Procedure For Estimating the Stress Intensity Factor of a Crack in a Finite Plate, Journal of Basic Engineering, 1964.

15. Conway, H. D., "The Approximate Analysis of Certain Boundary Value Problems, Journal of Applied Mechanics, 1960.

16. Hulbert, L. E., Hahn, G. T., Rosenfield, A. R., and Kanninen, M. F., "An Elastic-Plastic Analysis of a Crack in a Plate of Finite Size, Baltelle Memorial Institute, 1968.

17. Hooke, C. J., "Numerical Solution of Plane Elastostatic Problems By Point Matching," The Journal of Strain Analysis, 1968.

18. Paris, P., and Sih, G., "Stress Analysis of Cracks," Fracture Toughness Testing, ASTM STP-381, 1964.

19. Wnuk, M. P., "Review of Some Russian Papers Pertinent to the Fracture of Solids," National Aeronautics and Space Administration Research Grant No. NsG-172-60, GALCIT SM 67-9, 1967.

20. Savin, G. N., Stress Concentration Around Holes, Vol. 1, Pergamon Press, New York, 1961.

21. Hult, J. A. H., and McClintock, F. A., "Elastic-Plastic Stress and Strain Distribution Around Sharp Notches Under Repeated Shear," IXth International Congress of Applied Mechanics, Vol. 8, University of Brussels, 1957.

22. Hutchinson, J. W., "Singular Behavior at the End of a Tensile Crack in a Hardening Material," Journal of Mechanics, Physics and Solids, Vol. 16, 1968.

23. Fox, L., An Introduction to Numerical Linear Algebra, Oxford University Press, 1965.

24. Grobner, W., and Hofreiter, N., Integraltafel, Springer-Verlag, 1957.

The vita has been removed from the scanned document

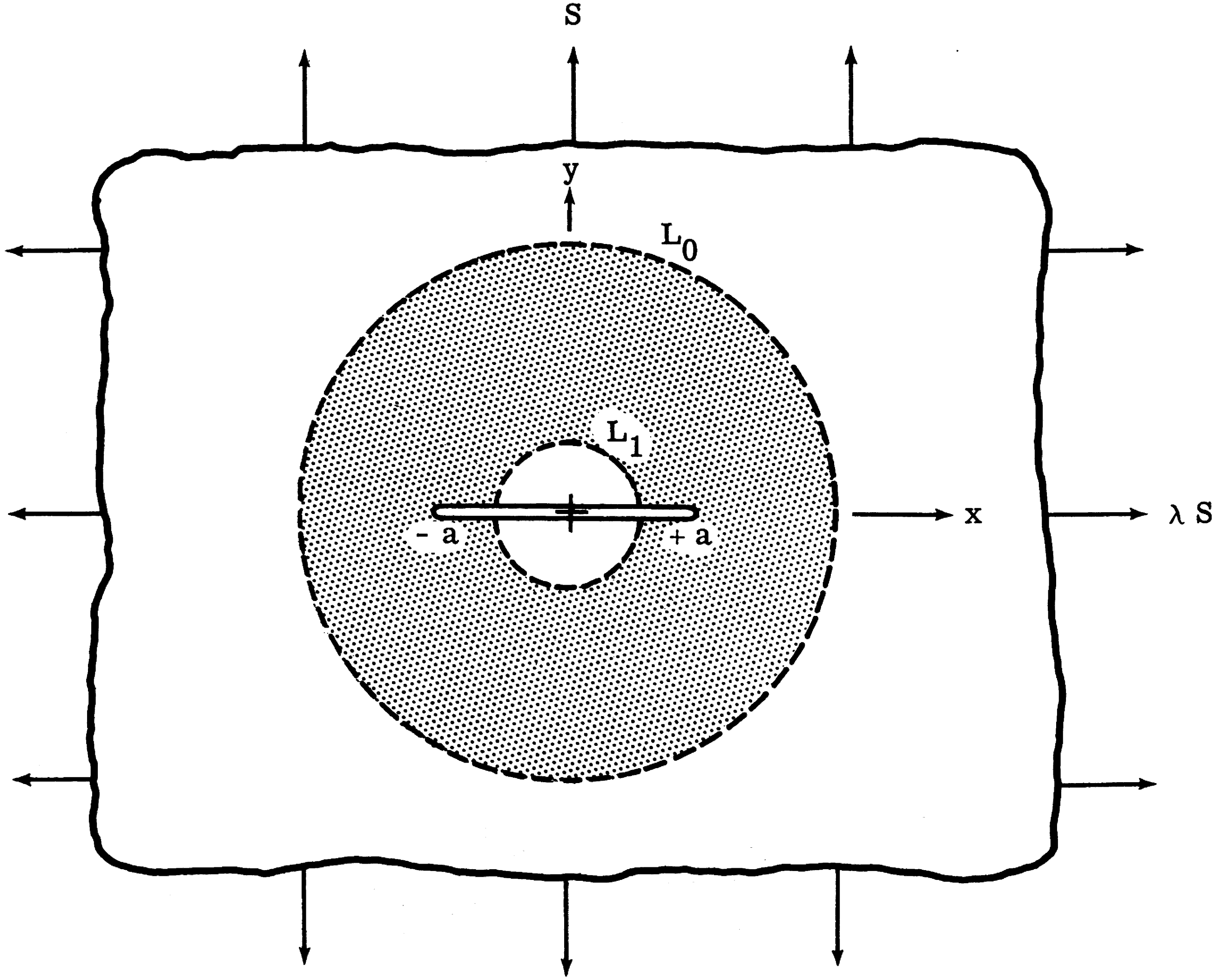

Figure 1.– Crack in an infinite plate subjected to a biaxial state of stress.

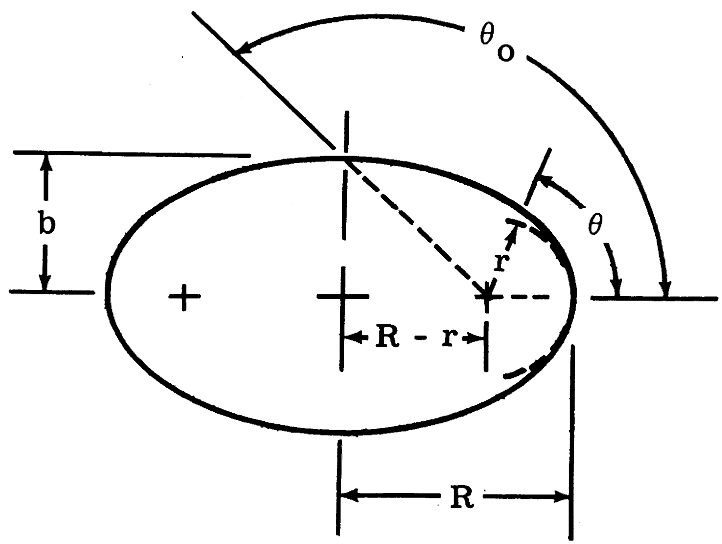

Figure 2.– Configuration used for determining the location of the collocation points for the circular and elliptic boundaries.

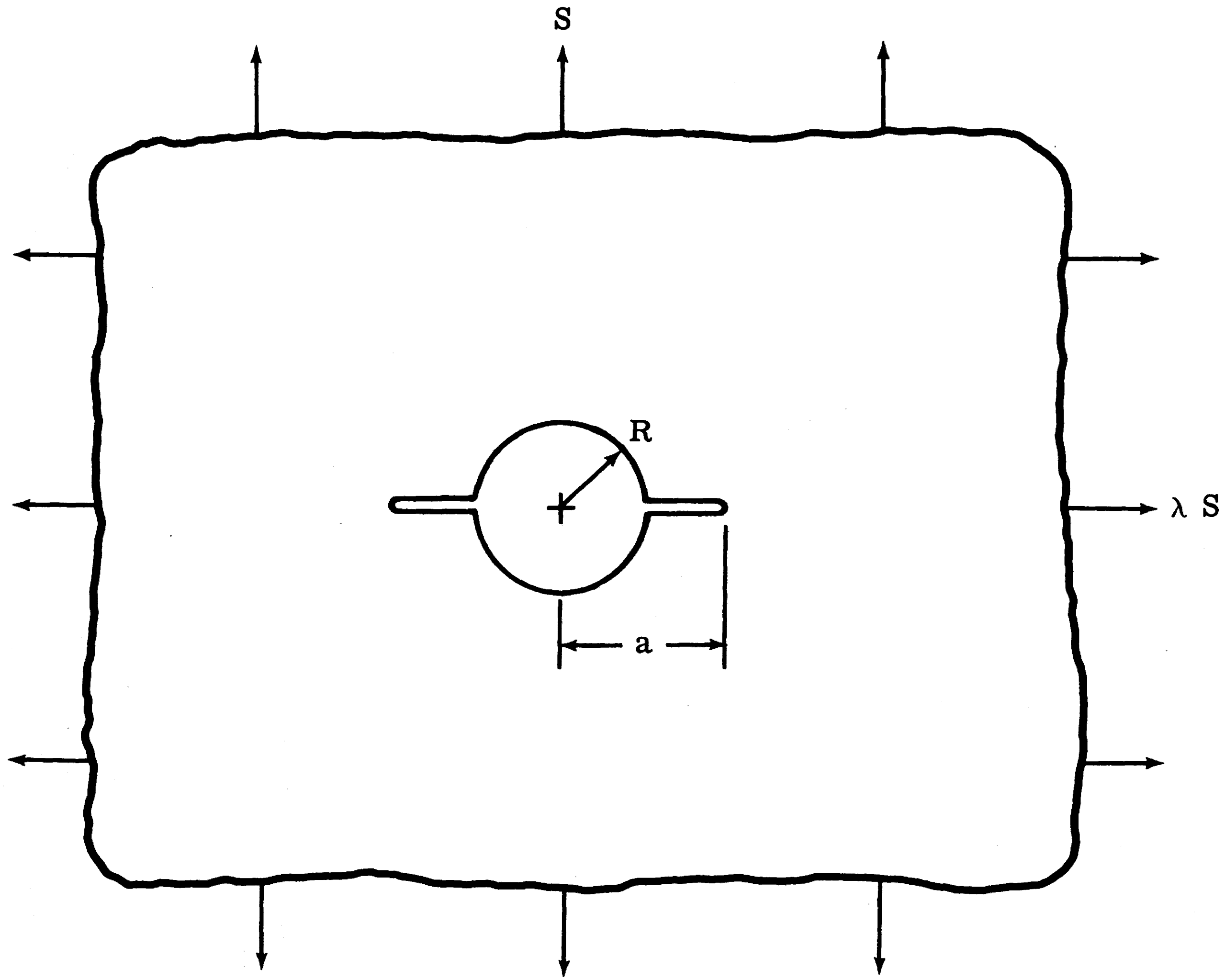

Figure 3.- Cracks emanating from a circular hole in an infinite plate subjected to a biaxial state of stress.

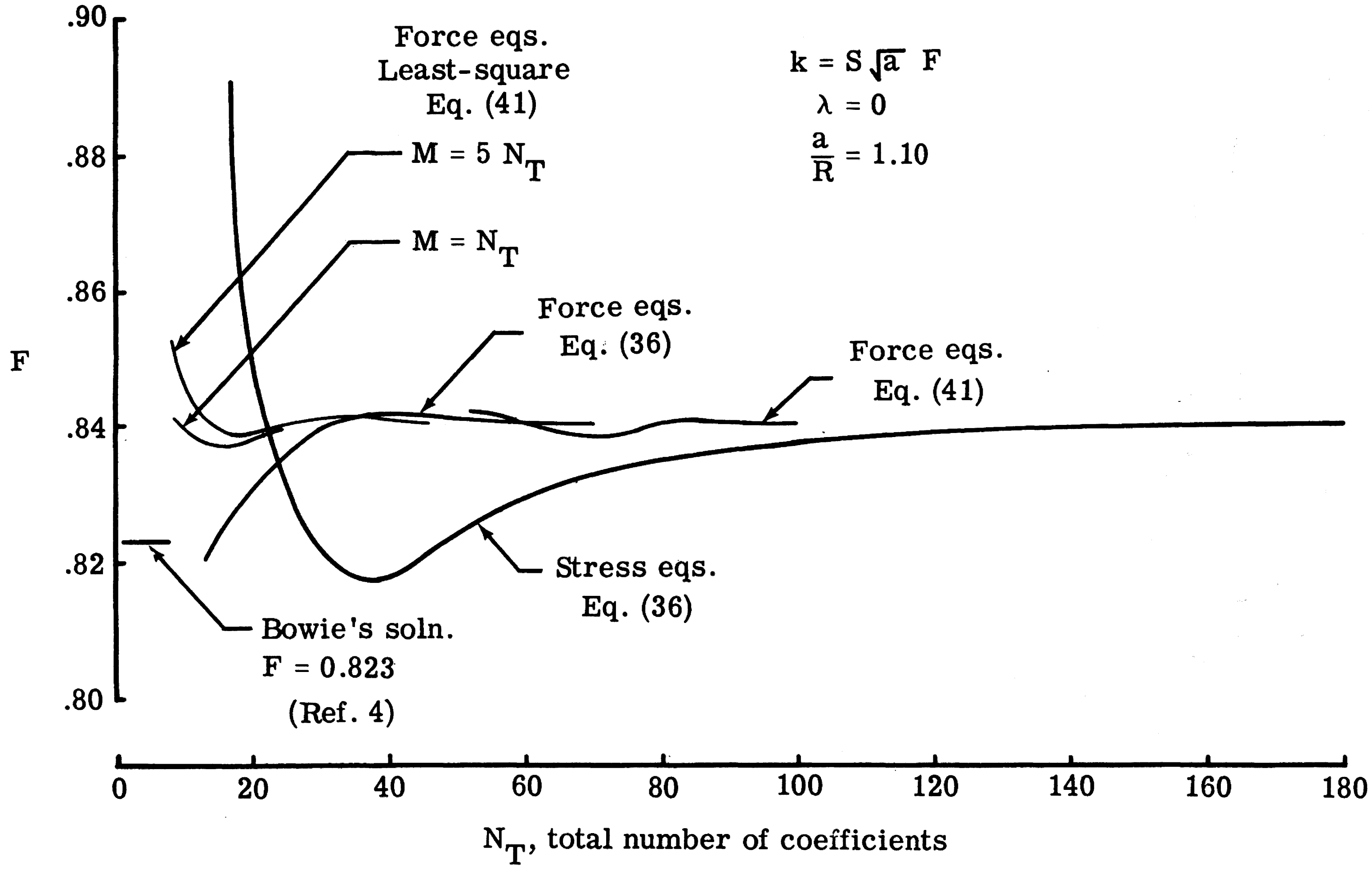

Figure 4.– Convergence curves for cracks emanating from a circular hole in an infinite plate subjected to a uniaxial state of stress.

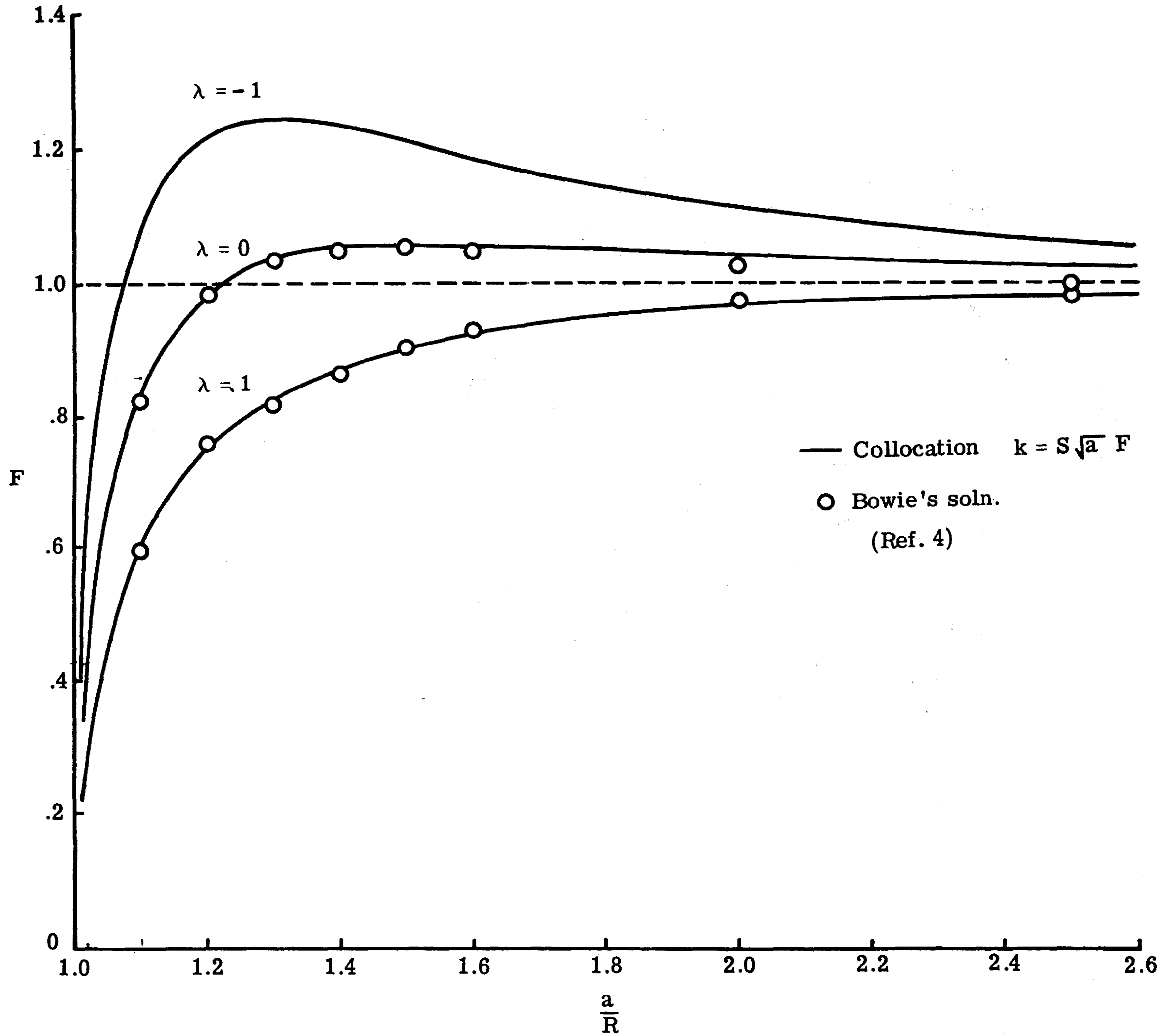

Figure 5.– Correction factor for cracks emanating from a circular hole in an infinite plate subjected to a biaxial state of stress.

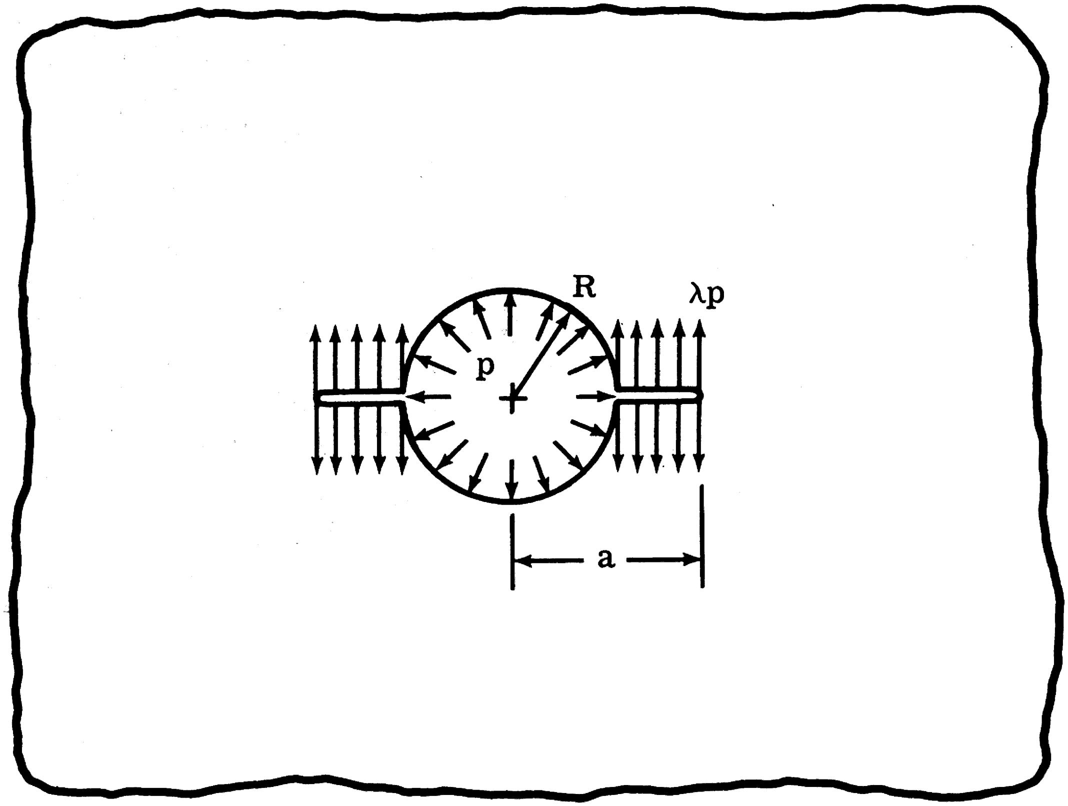

Figure 6.– Cracks emanating from a circular hole in an infinite plate subjected to internal pressure.

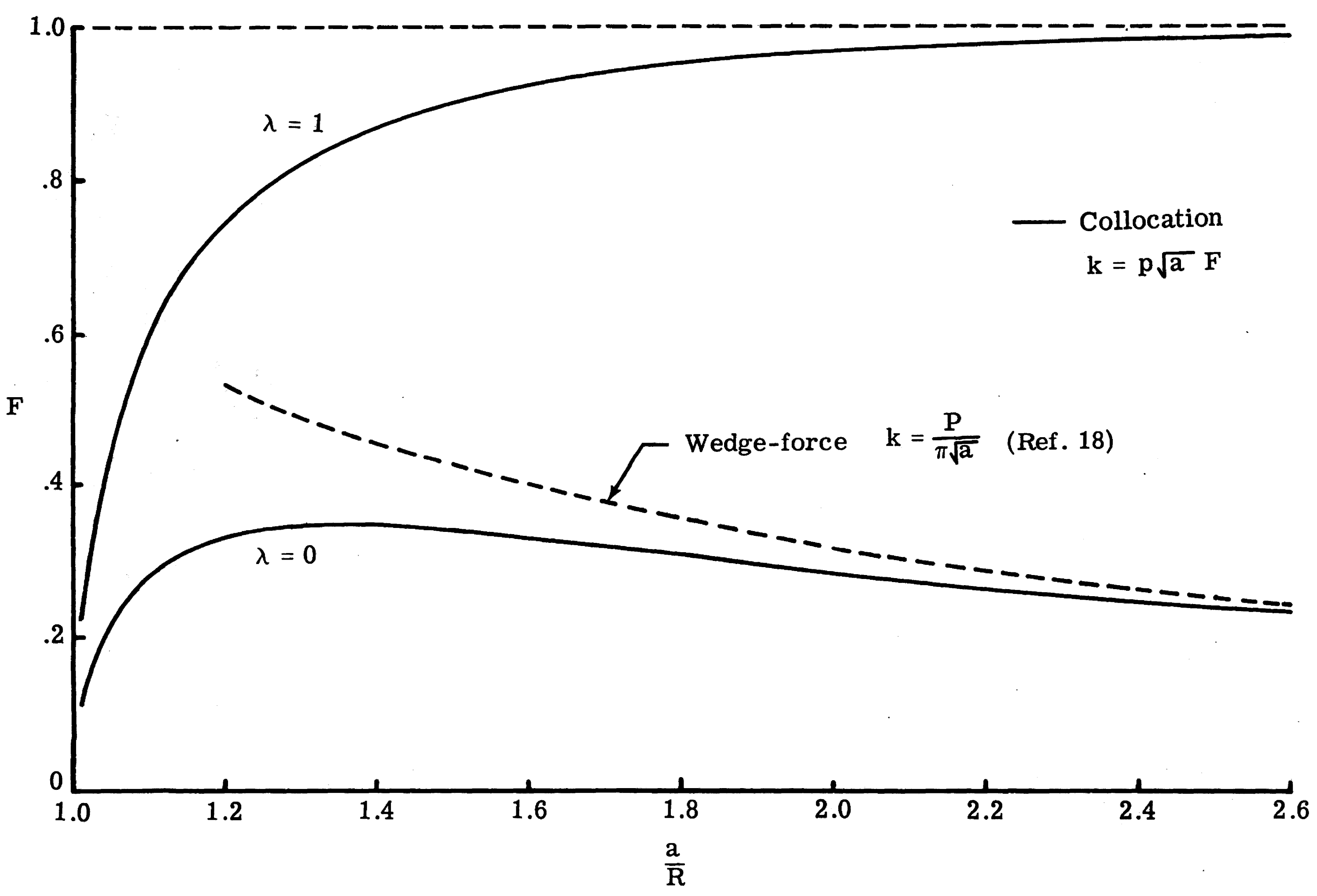

Figure 7.– Correction factor for cracks emanating from a circular hole in an infinite plate subjected to internal pressure.

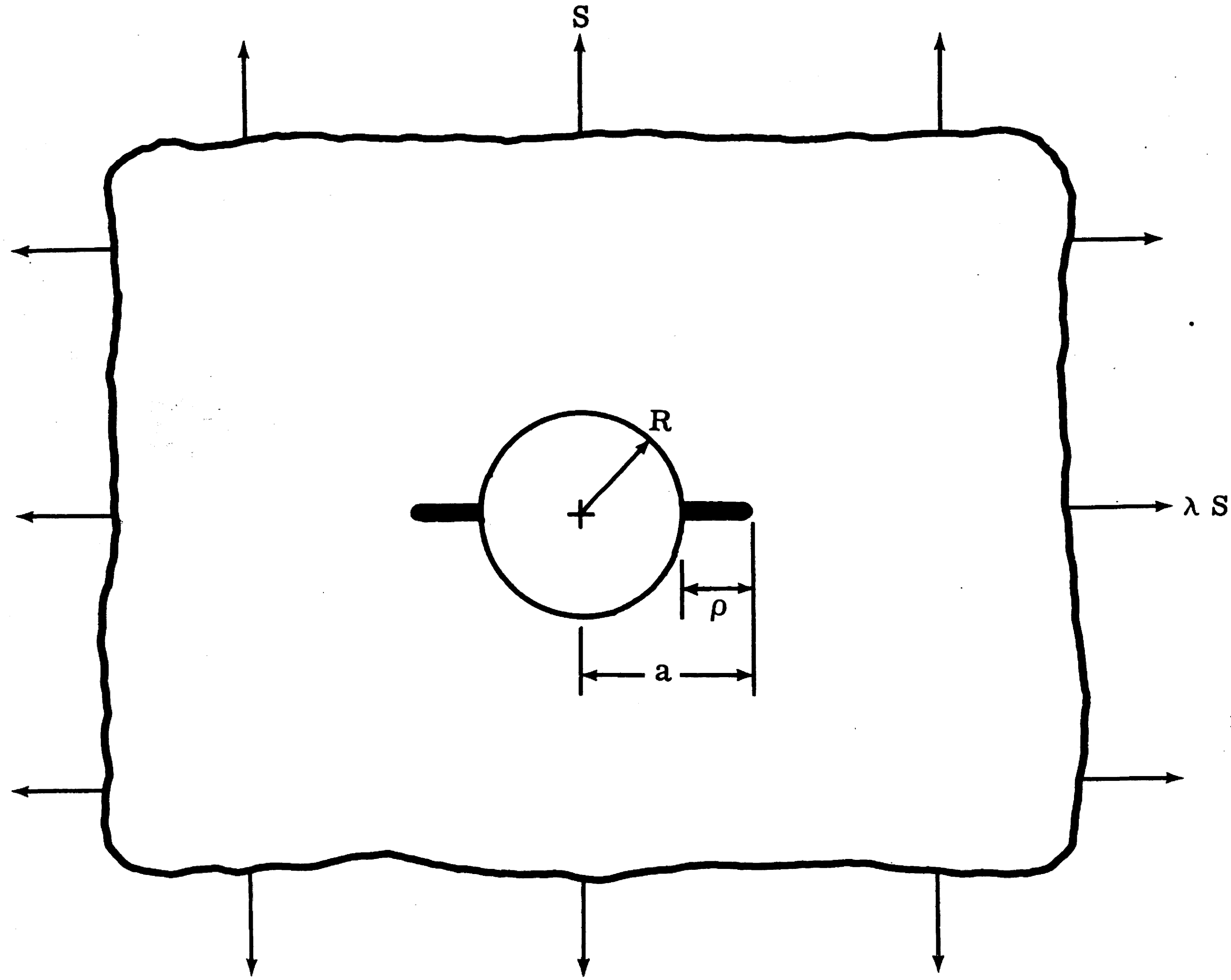

Figure 8.- Yielding from the edge of a circular hole in an infinite plate subjected to a biaxial state of stress.

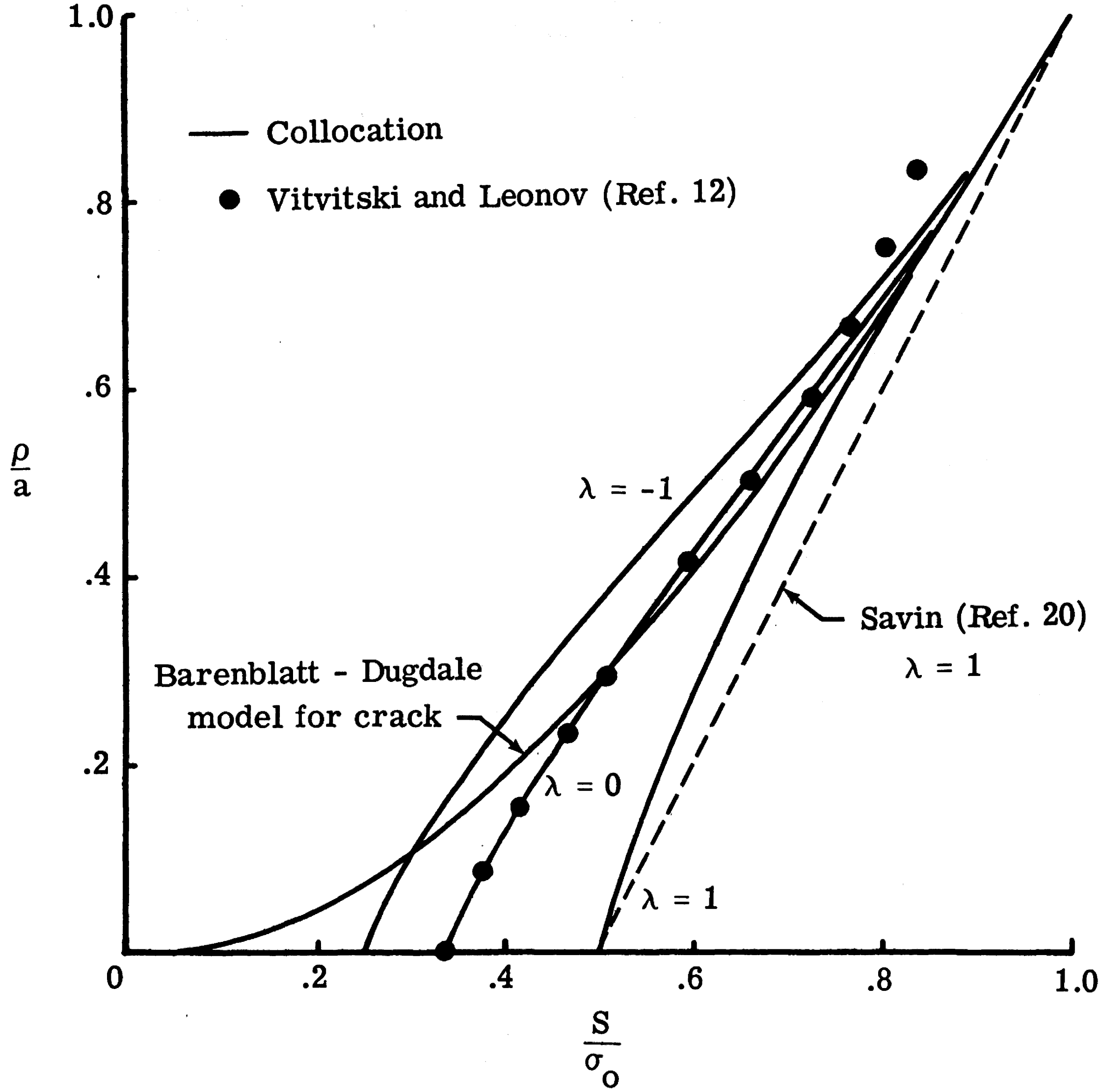

Figure 9.– Plastic zone length for a circular hole in an infinite plate subjected to a biaxial state of stress.

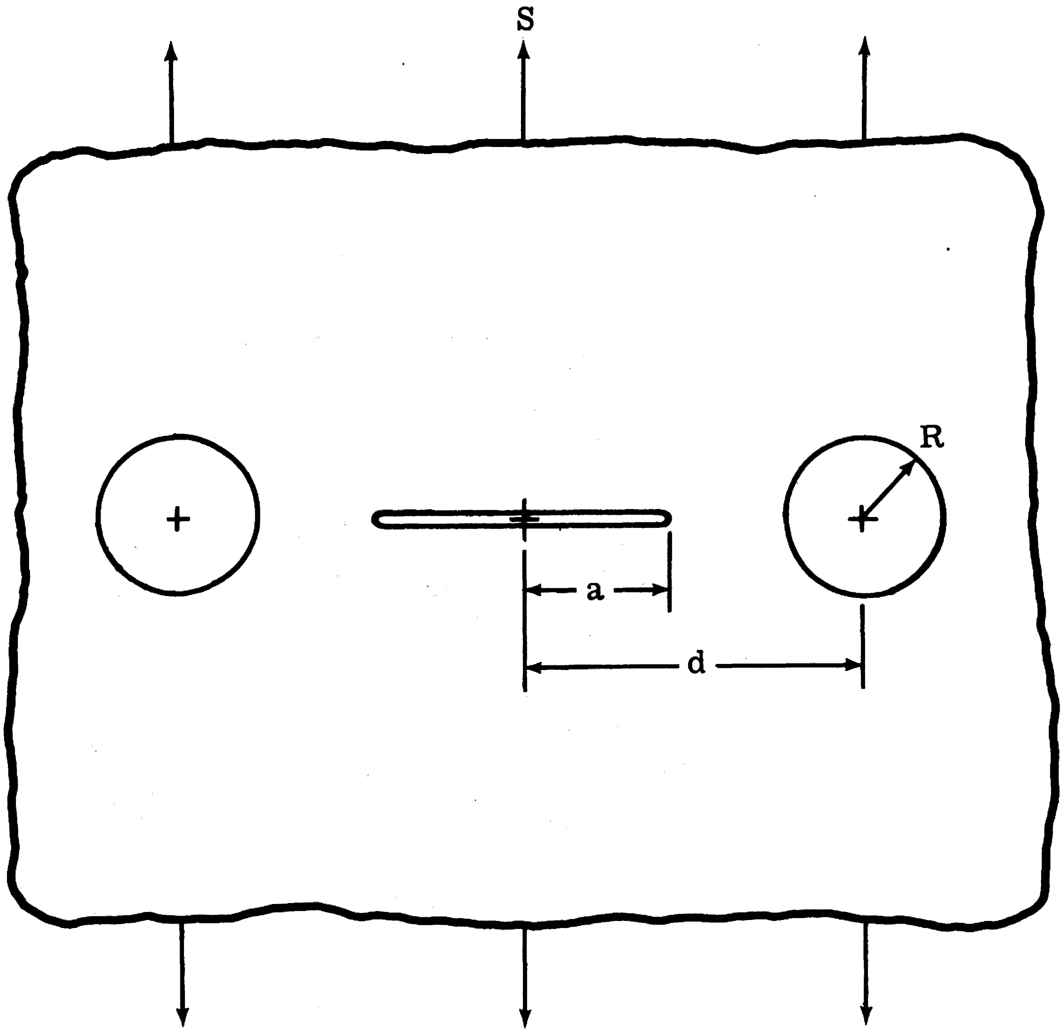

Figure 10.– Cracks approaching two circular holes in an infinite plate subjected to a uniaxial state of stress.

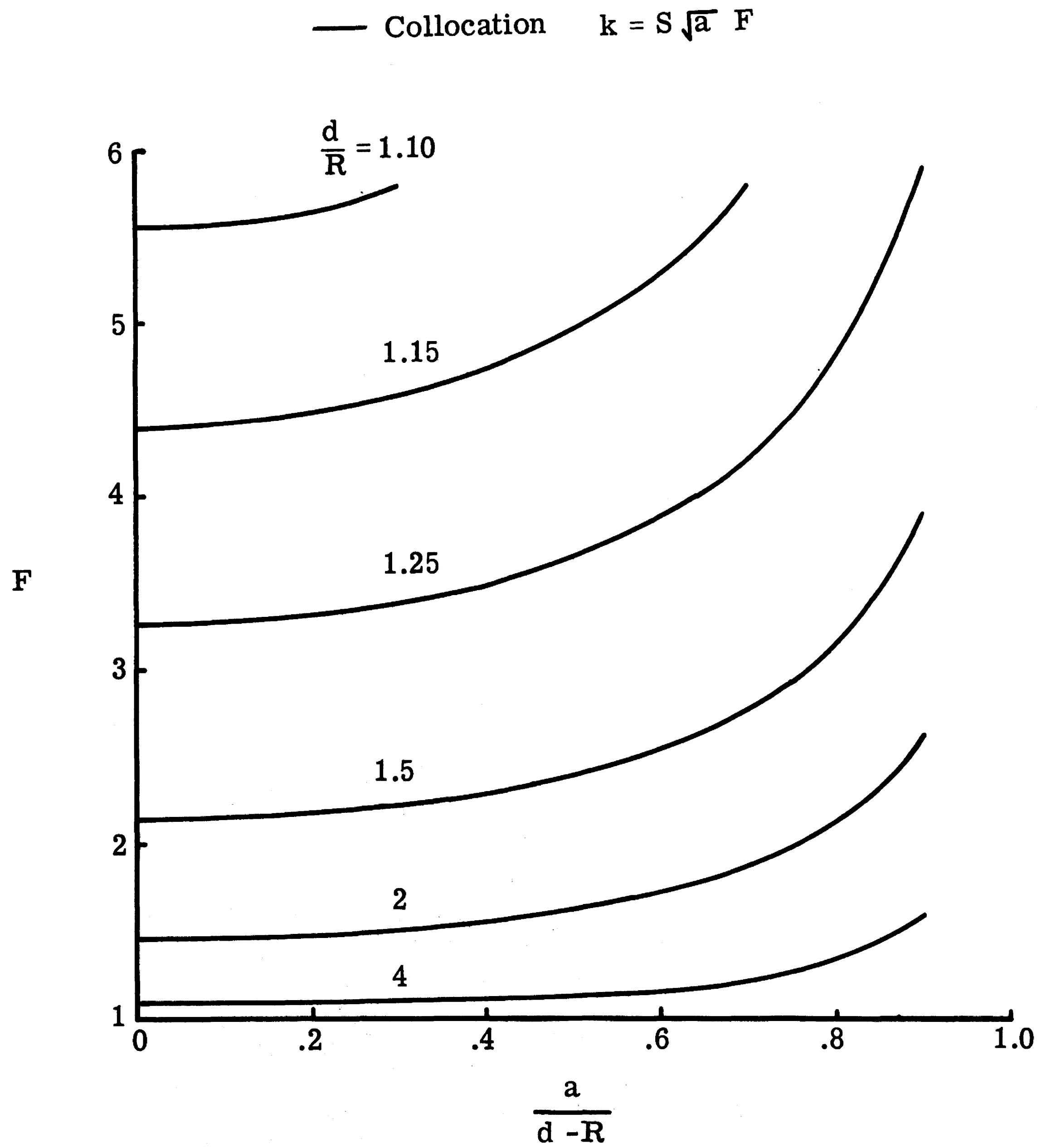

Figure 11.- Correction factor for a crack approaching two circular holes in an infinite plate subjected to a uniaxial state of stress.

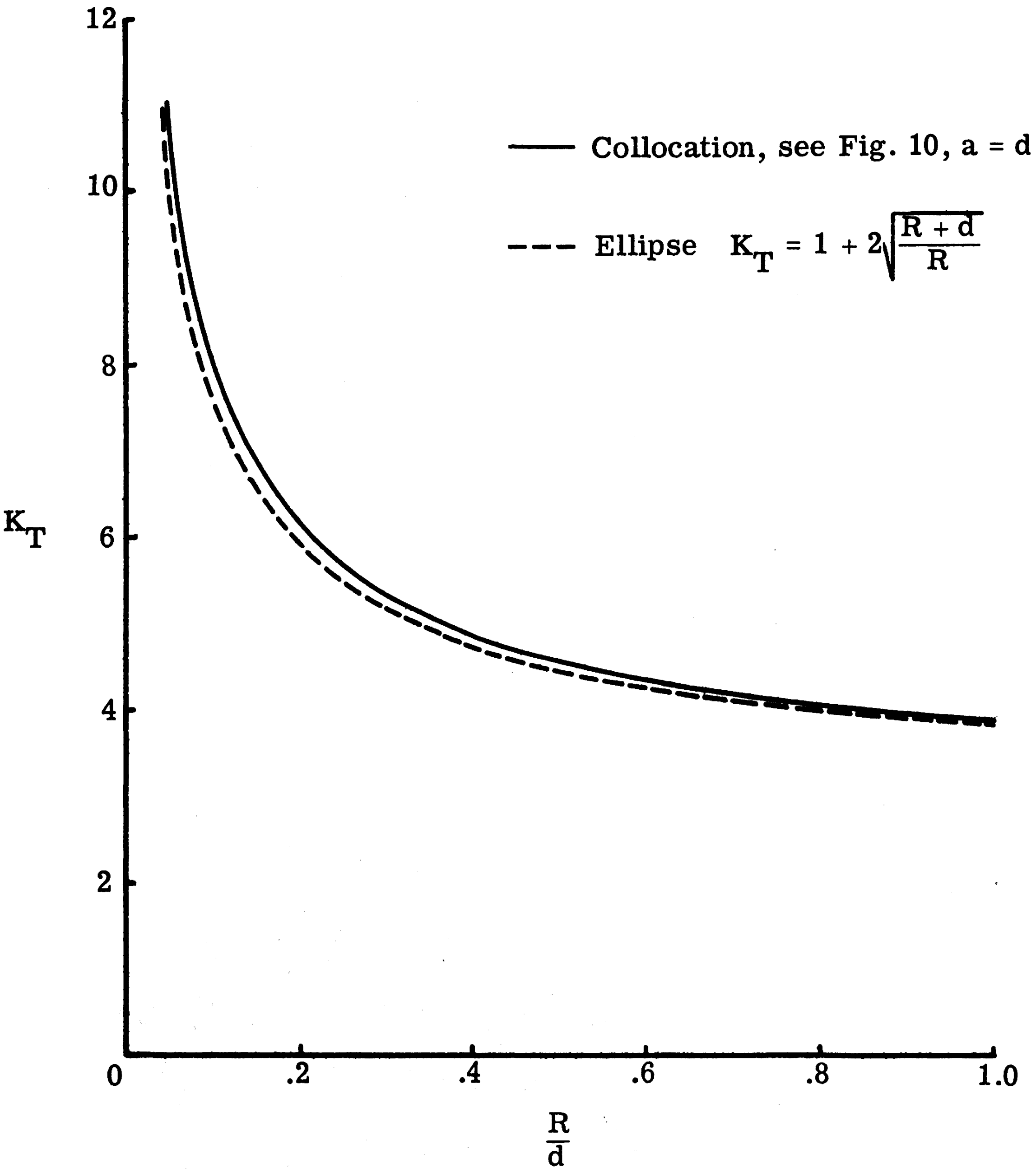

Figure 12.– Maximum stress concentration factor for two circular holes connected by a crack in an infinite plate subjected to a uniaxial state of stress.

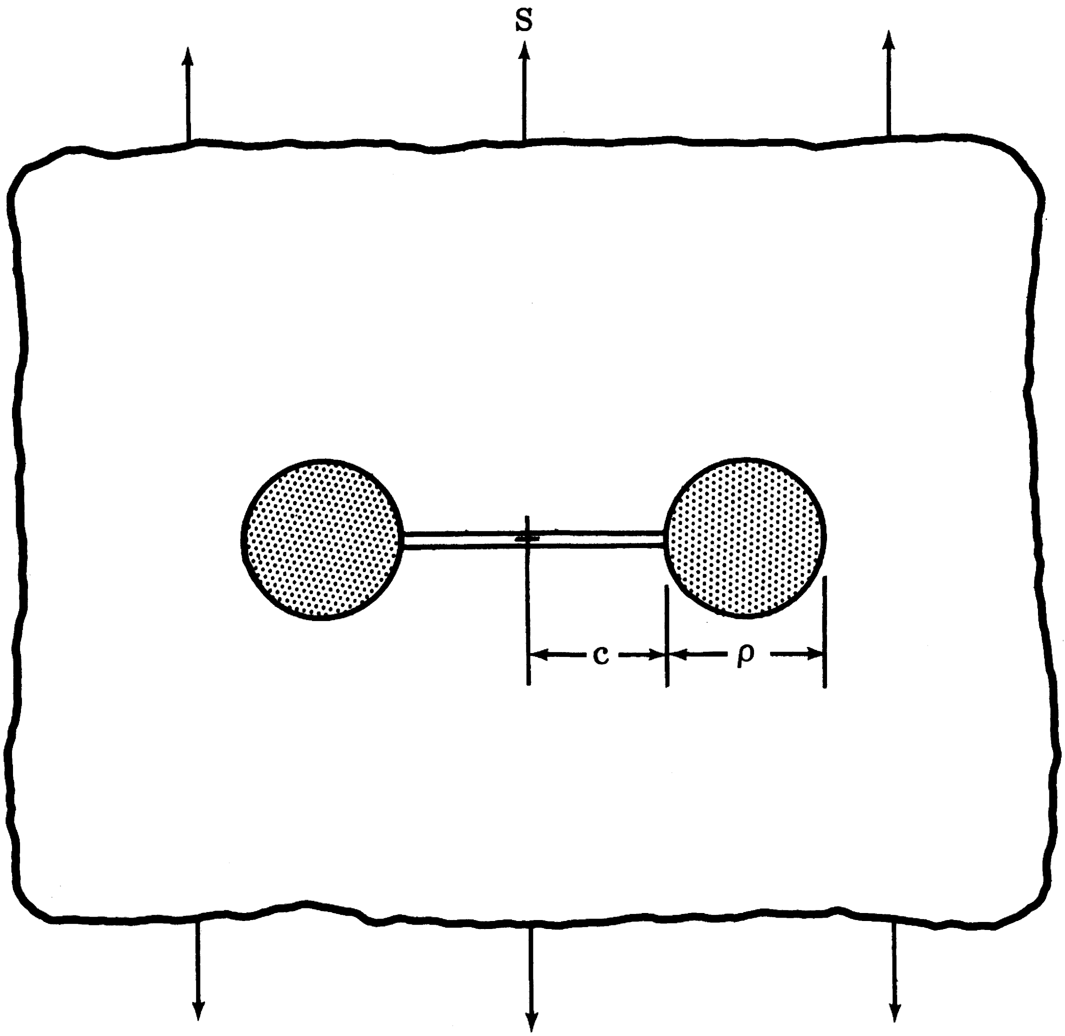

Figure 13.- Circular yield zones at the tip of a crack in an infinite plate subjected to a uniaxial state of stress.

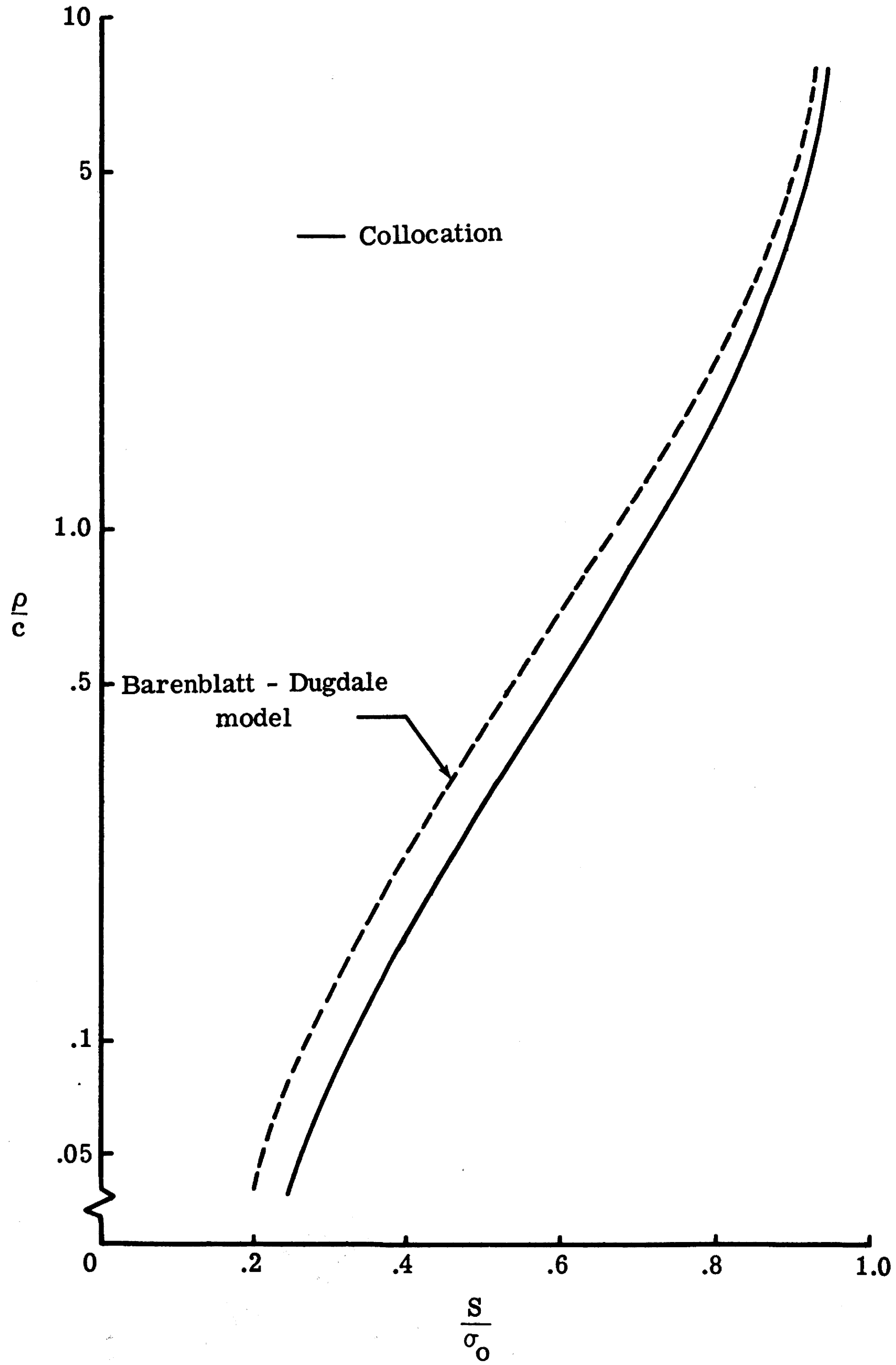

Figure 14.– Comparison of the plastic zone length for the Barenblatt–Dugdale model and the circular yield zone concept.

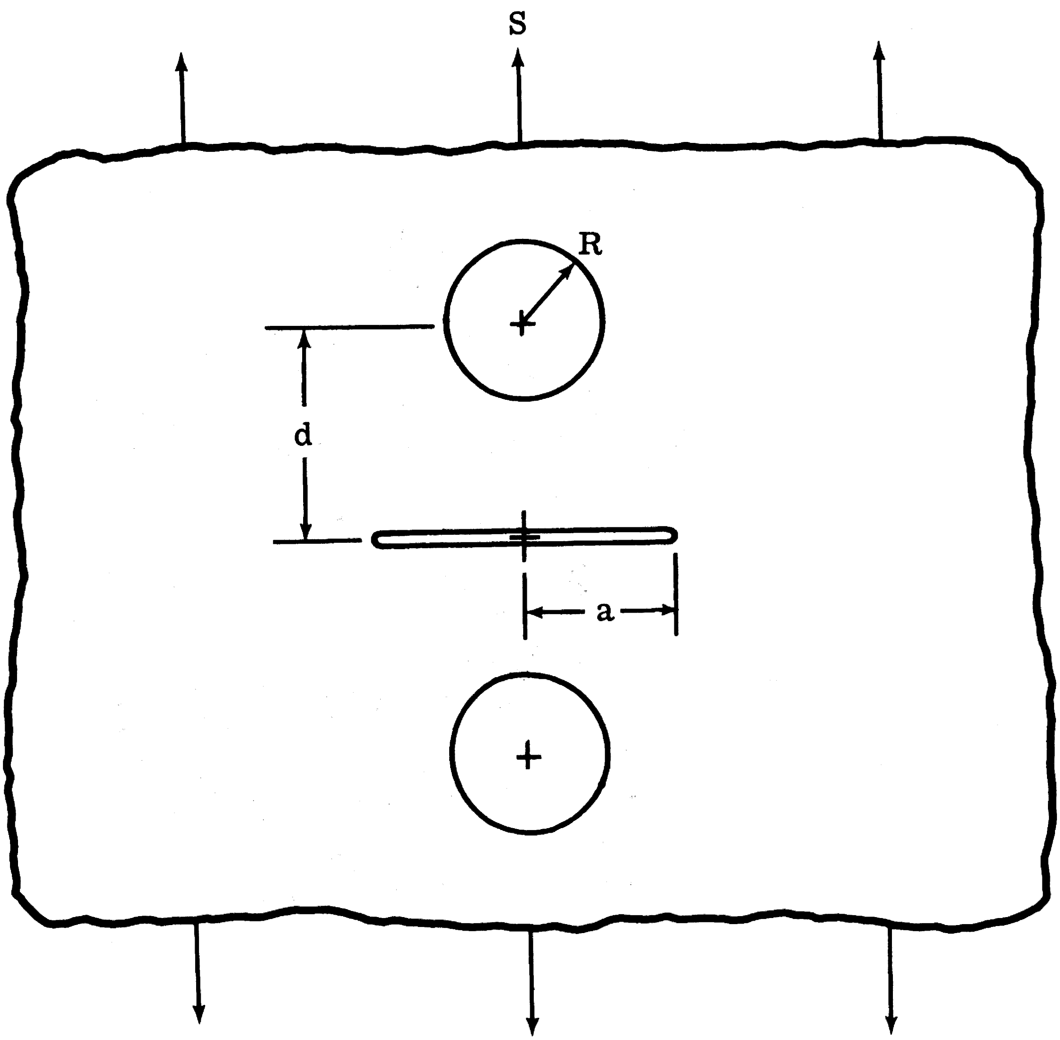

Figure 15.– Crack located between two circular holes in an infinite plate subjected to a uniaxial state of stress.

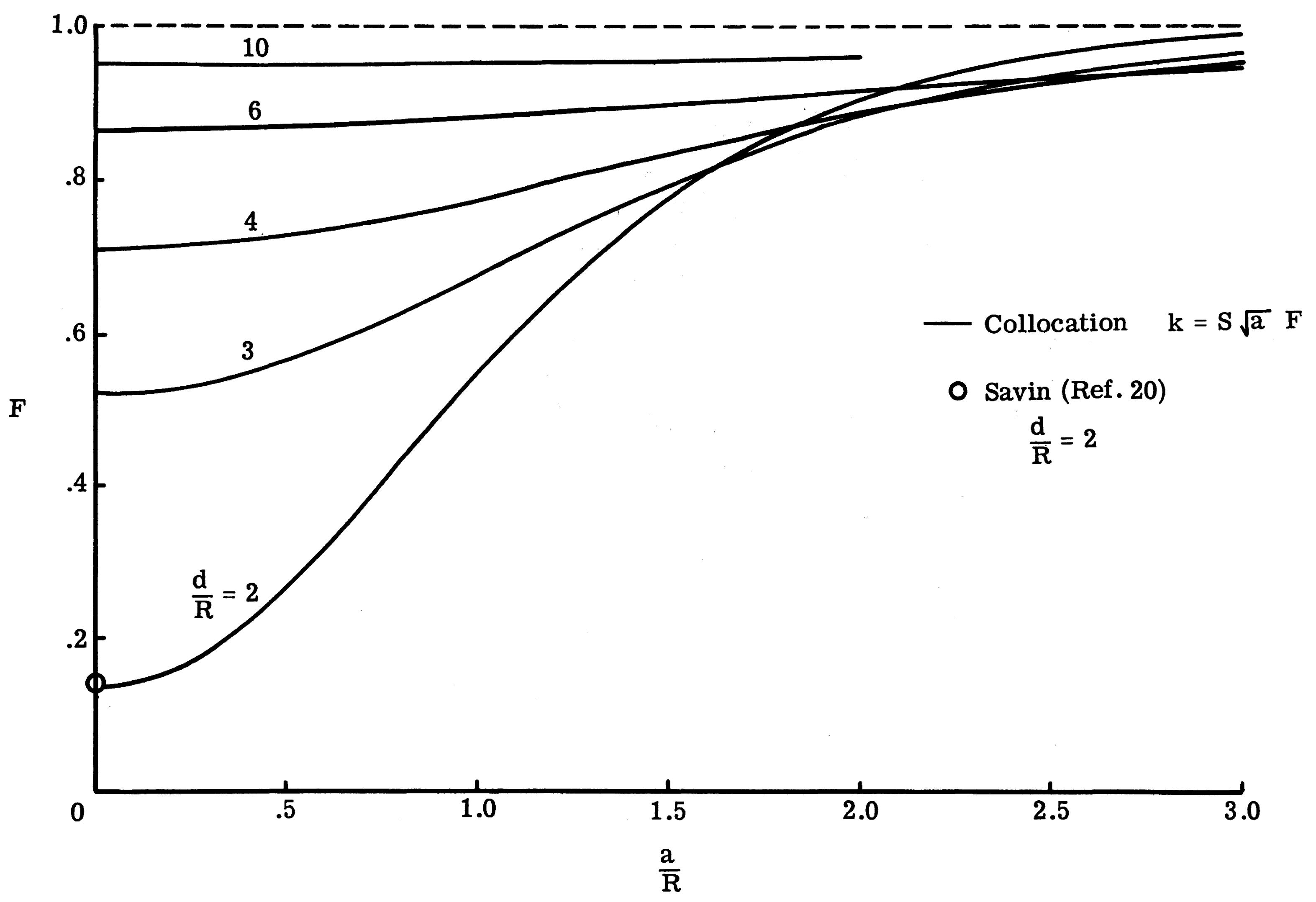

Figure 16.– Correction factor for a crack located between two circular holes in an infinite plate subjected to a uniaxial state of stress.

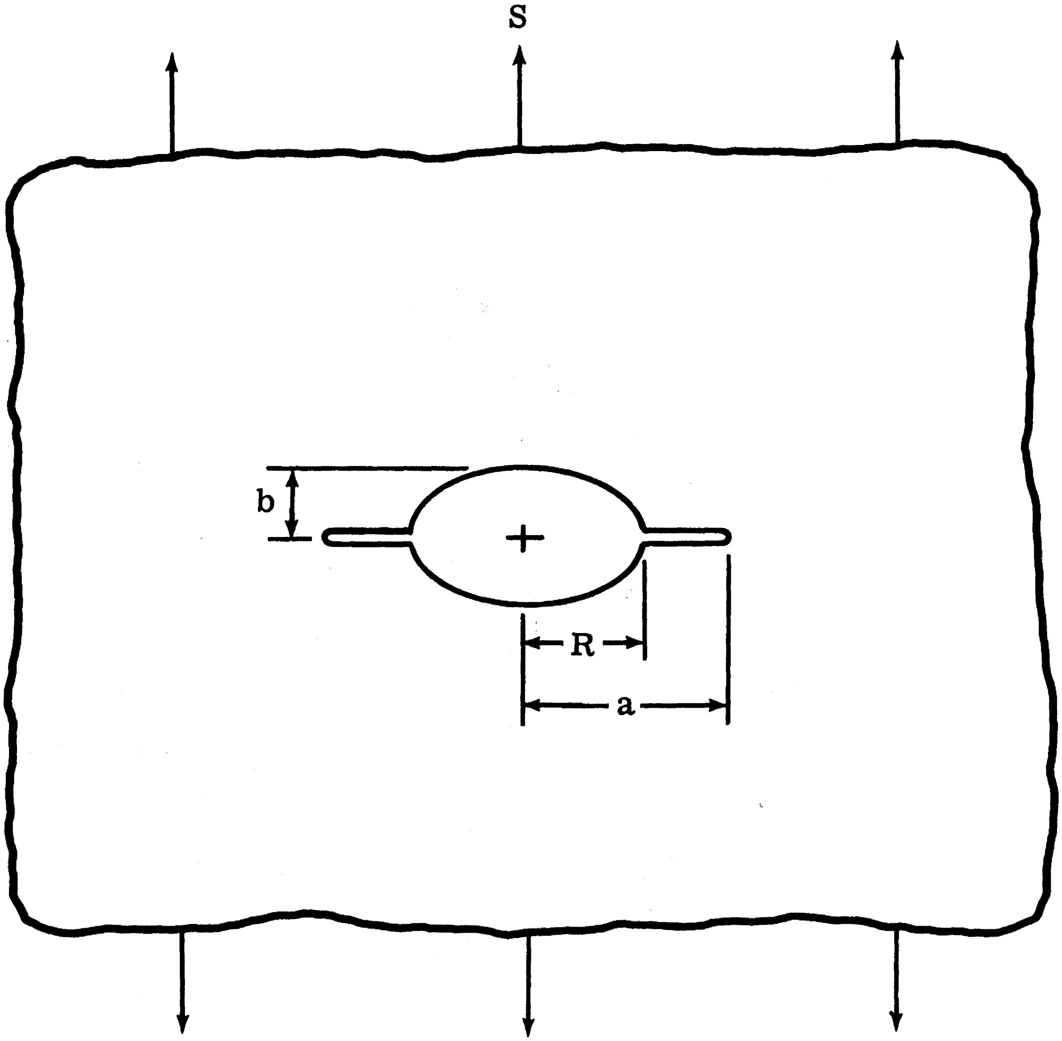

Figure 17.- Cracks emanating from an elliptical hole in an infinite plate subjected to a uniaxial state of stress.

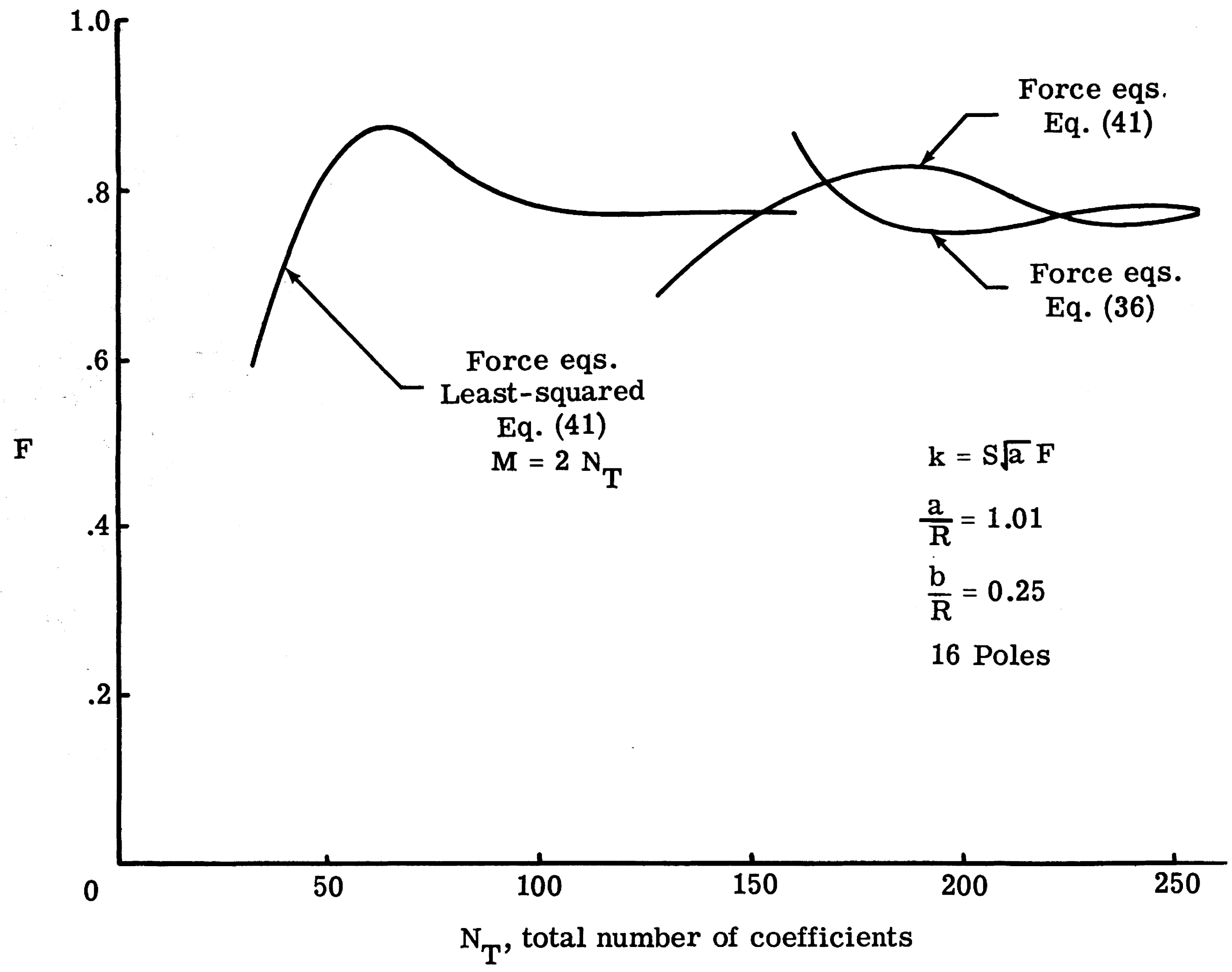

Figure 18.– Convergence curves for cracks emanating from an elliptical hole in an infinite plate subjected to a uniaxial state of stress.

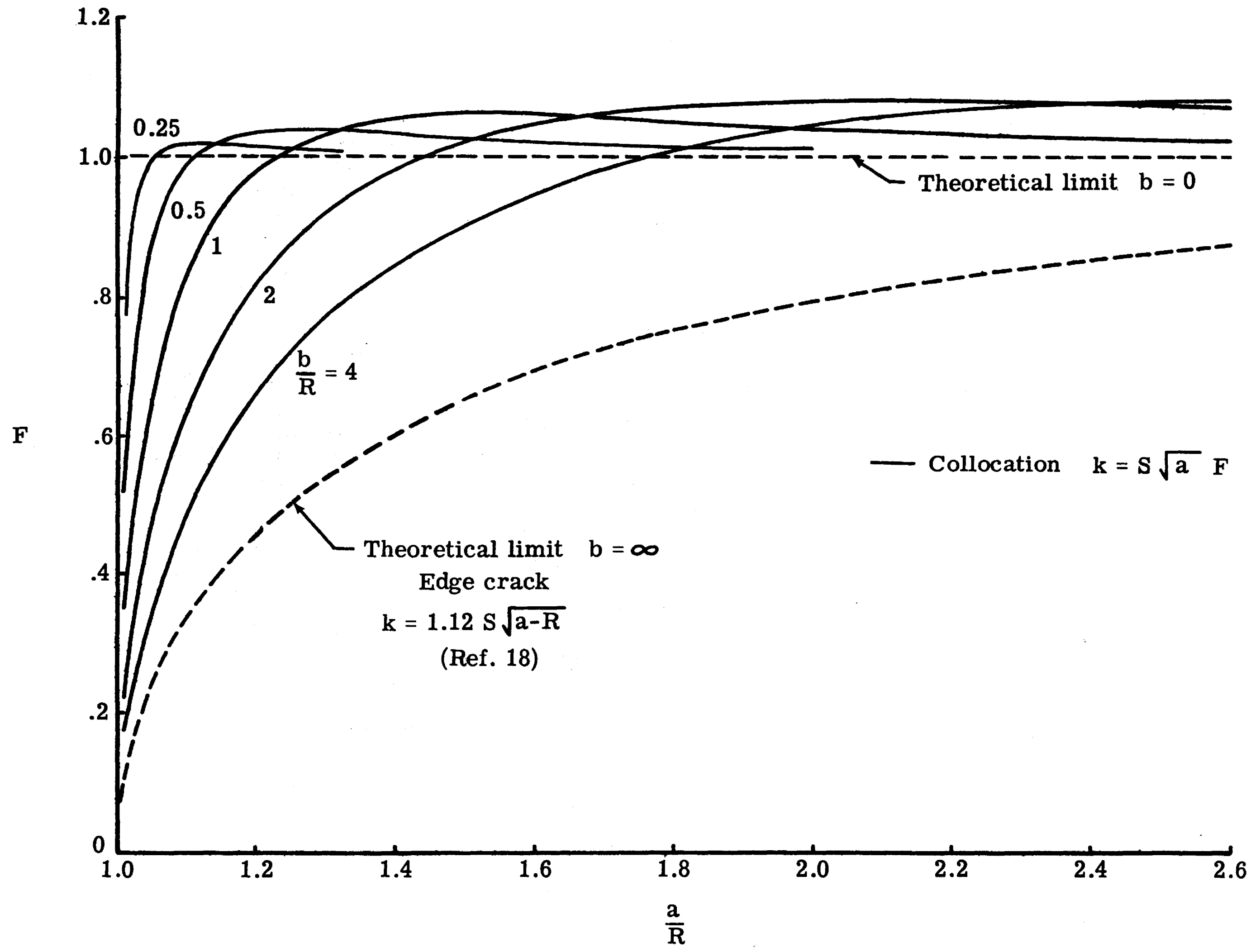

Figure 19.- Correction factor for cracks emanating from an elliptical hole in an infinite plate subjected to a uniaxial state of stress.

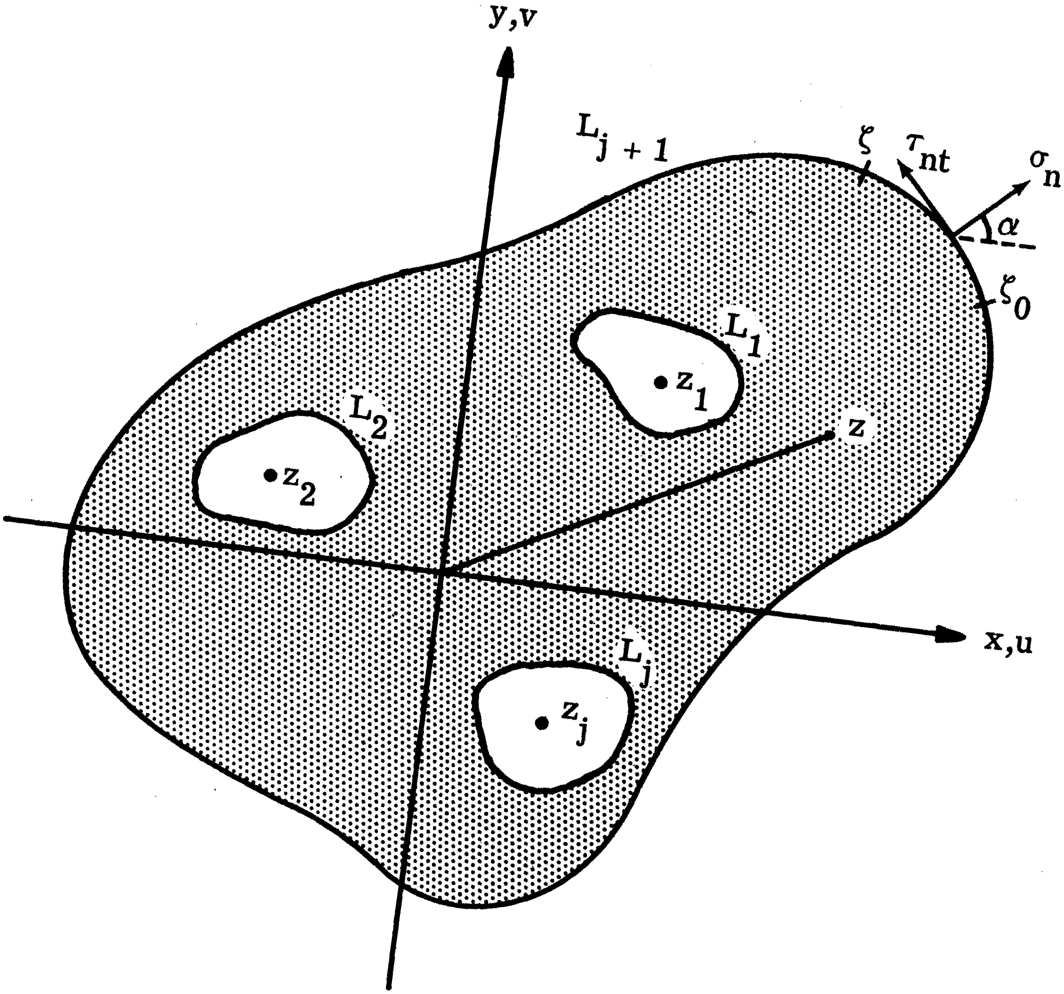

Figure 20.- Two-dimensional multiconnected body subjected to surface tractions.

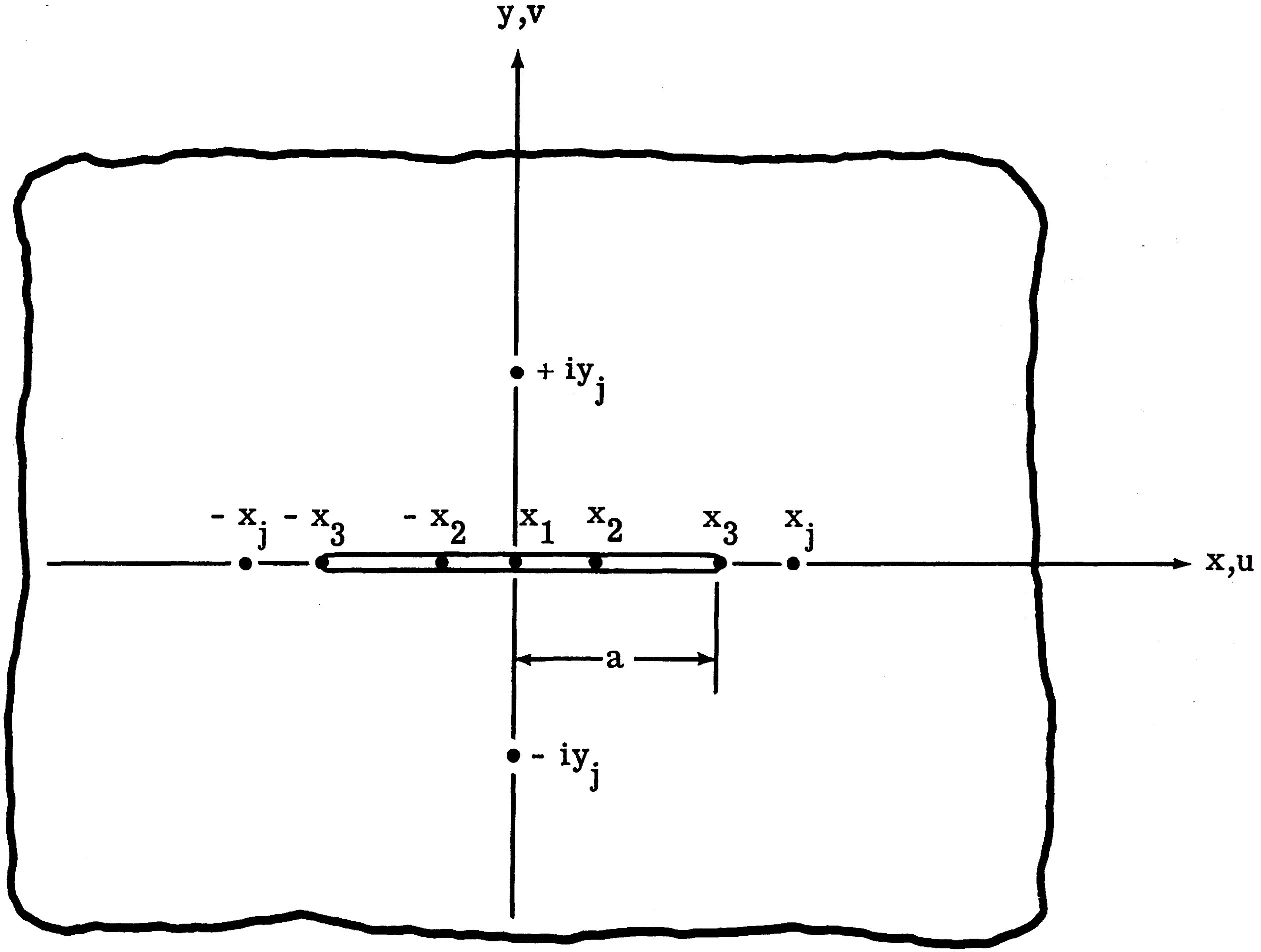

Figure 21.– Coordinate system used for the location of poles on the x and y axes.

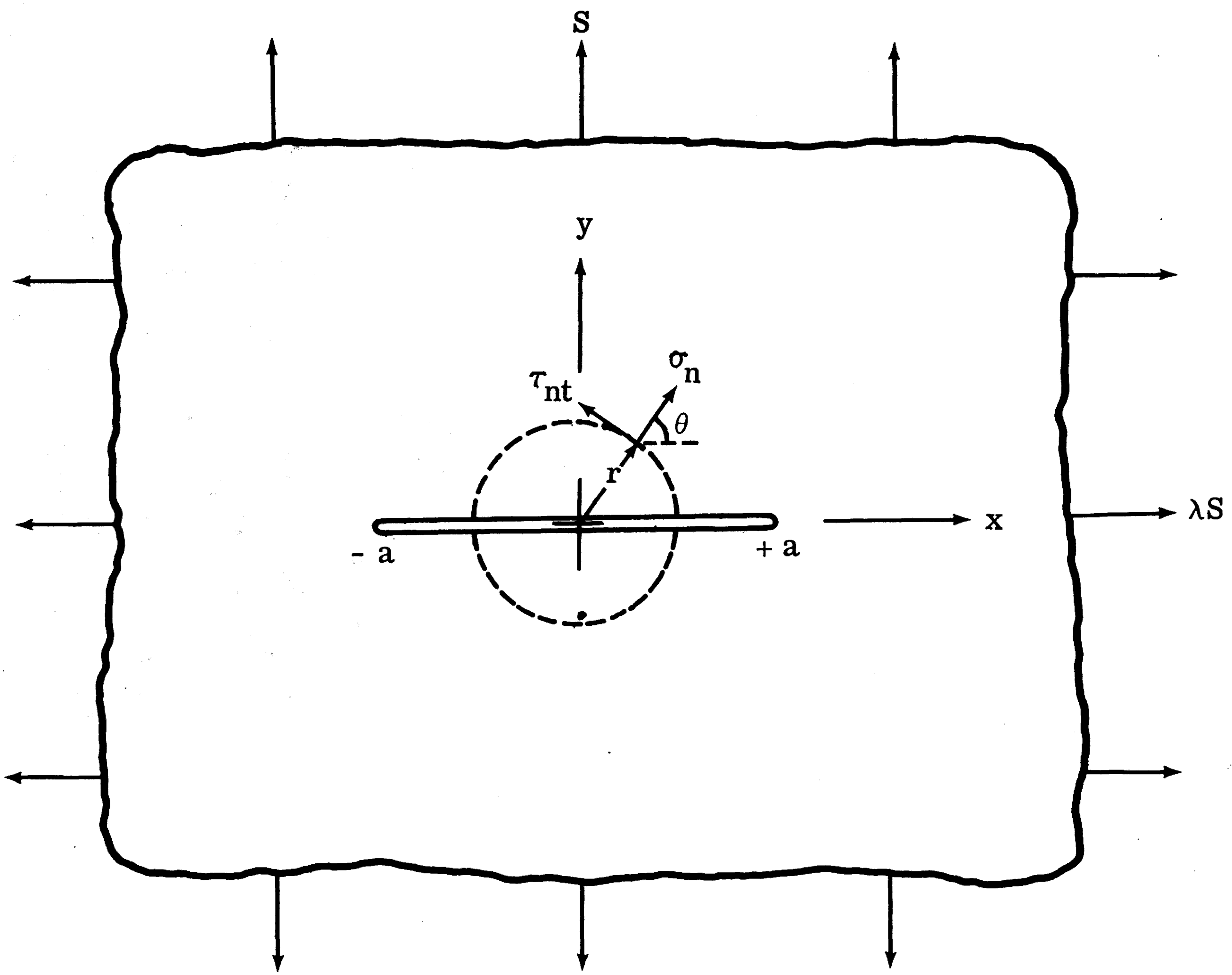

Figure 22.– Coordinate system used for the case of cracks emanating from a circular hole.

STRESS ANALYSIS OF SIMPLY AND MULTIPLY CONNECTED REGIONS

CONTAINING CRACKS BY THE METHOD OF

BOUNDARY COLLOCATION

By J. C. Newman, Jr.

ABSTRACT

Theoretical stress analyses were performed for the case of cracks emanating from, or in the vicinity of holes or boundaries of various shapes in two-dimensional elastic bodies. The solution is based on the complex variable method developed by Muskhelishvili and a numerical technique known as collocation for approximating the stress or displacement conditions on the boundary with appropriate series stress functions. These stress functions automatically satisfy the boundary conditions on the crack surfaces. The boundary collocation method included techniques such as, specifying stresses at equally spaced points on the boundary, specifying the resultant forces along arcs on the boundary, and a least-squares technique used to minimize the resultant force or displacement residuals along the boundary. The types of configurations investigated included the case of cracks emanating from a circular hole, the case of a crack in the presence of multiple-circular holes and the case of cracks emanating from an elliptical hole in an infinite plate. The configurations investigated were subjected to a variety of loading conditions. The results of the analyses are presented in terms of the crack tip stress-intensity factor.